EFFICIENT METHODS FOR INTEGRATED STRUCTURAL-AERODYNAMIC WING OPTIMUM DESIGN

by

Pi-Jen Kao

Dissertation submitted to the Faculty of the

Virginia Polytechnic Institute and State University

in partial fulfillment of the requirements for the degree of

Doctor of Philosophy

in

Aerospace and Ocean Engineering

APPROVED:

Raphael T. Haftka, Chairman

Bernard Grossman

Eric R. Johnson

Rakesh K. Kapania

John B. Kosmatka

March, 1989

Blacksburg, Virginia

EFFICIENT METHODS FOR INTEGRATED STRUCTURAL-AERODYNAMIC WING OPTIMUM DESIGN

by

Pi-Jen Kao

Raphael T. Haftka, Chairman

Aerospace and Ocean Engineering

(ABSTRACT)

The dissertation is focused on the large computational costs of integrated multidisciplinary design. Efficient techniques are developed to reduce the computational costs associated with integrated structural-aerodynamic design. First efficient methods for the calculations of the derivatives of the flexibility matrix and the aerodynamic influence coefficient matrix are developed. An adjoint method is used for the flexibility sensitivity, and a perturbation method is used for the aerodynamic sensitivity. Second a sequential optimization algorithm that employs approximate analysis methods is implemented. Finally, a modular sensitivity analysis, corresponding to the abstraction of a system as an assembly of interacting black boxes, is applied. This method was developed for calculating system sensitivity without modifying disciplinary black-box software packages. The modular approach permits the calculation of aeroelastic sensitivities without the expensive calculation of the derivatives of the flexibility matrix and the aerodynamic influence coefficient matrix.

Acknowledgements

A superior singer makes others follow his tune, and a superior educator makes others follow his idea. These few words are part of my feeling to my advisor, Dr. Raphael Haftka. I would like to thank him and Dr. Bernard Grossman for their guidance and support throughout this research. My gratitude is also extended to the faculty members of my doctoral committee: Dr. Eric Johnson, Dr. Rakesh Kapania, and Dr. John Kosmatka,

In addition I would like to express my sincerest appreciation to my wife,
whose patience and assistance helped me to finish the degree. My appreciation then goes to my mother and three sisters who have been a constant support and encouragement.

I certainly thank and . who performed the aerodynamic analysis involved in this project. Special thanks are extended to
for his performance calculations in the transport wing design. I am also grateful to

Dr. Rajiv Tharaja and Dr. Bruno Barthelemy for their help with the computer and for many valuable discussions.

I acknowledge the source of funding for this work: the National Science Foundation under grant DMC-8615336 and the NASA Langley Research Center under grant NAG-1-168.

This dissertation is dedicated to my late father.

Table of Contents

List of Illustrations

List of Tables

Chapter 1

Introduction

The design of an aircraft requires the integration of several disciplines, including aerodynamics, structures, control, and propulsion. Most traditional design optimization procedures are performed sequentially for a single discipline at a time. For example, aerodynamic specialists would first design a wing for optimum shape, and then structural analysts design the structure for minimum weight. The communication between the aerodynamic and structural designers has remained mostly at the conceptual design level where simple and cheap calculations are used. Otherwise, in preliminary and detail design, interactions are fairly rare except when they are forced to deal with aeroelastic phenomena such as flutter or loss of control effectiveness.

A study in Ref. 1 showed that the traditional sequential design procedure may lead to a suboptimal design compared with an integrated design procedure. The reason is that for each discipline, designers in a sequential decision-making process get in-

put from previous discipline design results, but lack the freedom to change that input. An integrated design procedure can improve a design in one discipline by design changes in another discipline. For example, structural weight can be reduced not only by changing structural design variables but also by modifying aerodynamic planform variables. Conversely, structural deformation can be used to minimize induced drag (Ref. 2). Although integrated design is more truly optimal than traditional sequential design, the difference in performance was not enough of an incentive to overcome the computational difficulties associated with design integration until two modern developments provided additional incentives.

The first technology advancement was the advent of composite materials which permit designers to tailor material properties to produce favorable aerodynamic-structural interactions. For example, in the design of the Grumman X-29A forward-swept-wing fighter, the divergence problem of a swept-forward wing associated with unfavorable geometric bending-twist coupling was reduced by tailoring the composite material to have favorable bending-twist coupling. The second technology advancement was the use of active control systems to improve structural performance. An application of this concept was the gust-alleviation system designed to extend the fatigue life of the B-52 bomber. Sensors measure gust loads on the wing, and control surfaces on the wing are deflected to cancel part of these gust loads. Other applications of control-structural interactions are reported in the recent NASA Symposia on Recent Experiences in Multidisciplinary Analysis and Optimization (Refs. 3 and 4).

The use of composite materials in aircraft design for affecting aeroelastic response is known as aeroelastic tailoring. The term has been defined as the creative use of

the anisotropic properties of composite materials to properly control aeroelastic deformations, so that designers can improve both structural and aerodynamic performance. In design optimization, this means that more design variables (ply orientation and ply thickness distributions) can be employed, and results in new concepts or possibilities in advanced aircraft design. Two recent review papers provide further information on aeroelastic tailoring (Refs. 5 and 6).

Over the past thirty years, a large number of general purpose computer codes have been developed for the various disciplines associated with design of aerospace vehicles. The NASTRAN finite element code is a typical example of a structural analysis code. The use of these general purpose computer programs is a major consideration in the integration of design procedure. It is practically impossible to integrate these various codes to a single program, and it is prohibitively expensive to write a program that will include all the disciplinary analyses. Instead, we need to integrate these disciplinary programs into team work while keeping their original independence. If we want to preserve the autonomy of disciplinary optimization, we can organize a multilevel approach in which a system level optimization coordinates many subsystem optimizations (Refs. 7 to 13). The coupling between higher and lower levels often requires sensitivity of the optimum solutions of the subsystems.

An example of this approach shown in Fig. 1 is a three-level decomposition of a transport aircraft wing design (Ref. 13). The top level analyzes the mission and performance of the aircraft to minimize the fuel consumption. The middle level performs a finite element analysis of the wing box to minimize cumulative constraints which measure the load carrying capacity of each wing panel. The bottom level runs a de-

tailed stress and buckling analysis to minimize a cumulative constraint which represents the behavior response for a given set of loads.

Another approach is to use a single optimizer to couple the analysis modules of different disciplines. An objective function is chosen to reflect the most important design objective such as minimum weight or maximum range. Disciplinary analysis programs are called within the optimizer to calculate constraints and their sensitivity derivatives. Communication between disciplines is achieved by calculation of sensitivities of the response of one discipline to input coming from other disciplines. This approach is taken in the present work.

No matter what scheme is used to integrate multidisciplianry design optimization, the computational costs are enormous due to the need to repeatedly call large computer programs. The present work is part of an ongoing project on the combined aerodynamic/structural design of aircraft wings, which is presently on reducing the computational costs associated with multidisplinary design.

Initially, a simple sailplane was chosen to examine the interactions between aerodynamic and structural design. The overall objective function of the aerodynamic design was to maximize the cross-country speed of the sailplane. The objective of the structural design was to minimize the weight. The simplicity of the sailplane allowed for the use of simple analysis methods; lifting-line theory was used for the aerodynamic analysis and beam theory was used for structural analysis. Two optimization procedures were compared. The first is a sequential, iterative approach representing a traditional aircraft design, and the second is an integrated approach.

The results (Refs. 14,15) indicated that the integrated design achieved a lower weight and improved aerodynamic performance over the sequential, iterative design.

The second goal of the research was to investigate the computational costs and develop efficient methods of integrated design for the same sailplane. We replaced the simple analysis methods of beam theory and lifting-line theory with more refined models which are a finite element method for the structural analysis and a vortex lattice method for the aerodynamic analysis. The aeroelastic analysis is based on the assumption that only torsional deformations have significant aeroelastic effect. Two matrices are then defined to represent interactions between the structure and the aerodynamics. One is an aerodynamic influence coefficient matrix which represents the change in lift coefficient at one chord due to a unit twist in another chord. Another is a structural flexibility matrix which represents the change in twist angle at one chord due to a unit load at another chord. Although only 80 vortex panels are used to calculate aerodynamic responses, and 270 degree of freedoms are used to get structural responses, the computational costs associated with design optimization were still quite high due to the need for calculation of the sensitivity derivatives of these two matrices. Ten hours CPU time on IBM 3084 had been estimated for a complete design without efficiency improvements. Using approximate optimization procedures and efficient sensitivity calculations, this time was reduced to less than ten minutes (Ref. 16).

The next stage was to develop an integrated wing design procedure for a subsonic transport aircraft. The finite element structural model and the vortex lattice aerodynamic model of a transport wing are more expensive than the sailplane wing models, and additional reduction in computation costs is required. One way to

achieve that is to use a modular sensitivity analysis which is based on Ref. 17. In this approach, a system level sensitivities are computed from subsystem derivatives. This approach is more efficient because it does not require the derivatives of the aerodynamic influence coefficient matrix and the flexibility matrix (Ref. 18).

This dissertation presents the results of the last two stages in the research effort with special emphasis on the structural and aeroelastic analyses for which the author was responsible. Additional details for the aerodynamic analysis are available in Refs. 19 and 20.

Chapter 2 presents the integrated design of the sailplane wing using a finite-element analysis for the structure and a vortex-lattice method for the aerodynamics. Efficient methods for cross-sensitivity calculations and approximate optimization procedures are presented as a way to reduce computational costs.

Chapter 3 presents the integrated design of a transport wing modeled by the finite element and vortex lattice methods. A modular sensitivity formulation is developed. Sensitivity results are compared with a forward finite difference scheme.

Chapter 2

Sailplane Wing Design

The objective of the sailplane wing design was to investigate the computational costs of multi-disciplinary design. We used more realistic panel methods for the aerodynamic loads on the wing and a finite-element analysis of the wing structure. In order to reduce our computational effort we utilized only 80 panels for the aerodynamic model and 270 degrees of freedom for the structural model. These models, although simpler and cheaper to analyze than typical design models, were still much more expensive than the rudimentary models used in our previous research (Ref. 15).

2.1 Analysis

2.1.1 Structural Model

The structural details of the sailplane wing cross section are shown in Fig.2. The skin and the spar webs are of a sandwich construction of Kevlar face sheets with a foam core. The main spar is an I-beam with spar caps built of unidirectional graphite fibers oriented spanwise. The structural analysis was performed using a modified version of the finite element program WIDOWAC (Ref. 21). Eight aerodynamic chords were used for the computation of the aerodynamic loads, and Fig. 3 shows their locations along the wing span and the grid points for a typical cross-section. The aerodynamic force is applied at the aerodynamic center, for example, grid point 7. The model has 270 degrees of freedom and 409 elements. There are 192 anisotropic 4-node quadrilateral membrane elements to model the skins which were stacked up of 0^0, $\pm$ 45^0 and 90^0 plies. Seventy-six shear web elements model the spar webs. The remaining elements are bar elements which model the spar caps and the vertical stiffness of the ribs and spar webs. The material properties of the Kevlar/epoxy are E1 = 76.0 GPa, E2 = 5.5 GPa, ν_{12} = 0.34 and G12 = 2.3 GPa. The material properties of the graphite/epoxy are E1 = 203.0 GPa, E2 = 11.2 GPa, ν_{12} = 0.32 and G12 = 8.4 GPa.

2.1.2 Aerodynamic Model

The planform of the high aspect-ratio sailplane wing is shown schematically in Fig. 4. The four parameters x_6 - x_9 represent planform design variables. Two other aerodynamic design variables are the twist angles at the break and the tip (relative to the root). The airfoil section, for all spanwise stations is the Boeing BoAR-80-RPVT-16B, described in Ref. 14. The aerodynamic analysis is based on a vortex-lattice method(VLM), such as discussed in Ref. 19. In this approach, the continuous distribution of bound vorticity over the wing surface is approximated by a finite number of discrete horseshoe vortices that are placed in trapezoidal panels. For the simple configuration in the sailplane design we used a total number of 80 panels, (8 spanwise, 10 chordwise) to model the wing. The lift and induced drag are computed from the integrated circulation distribution. The profile drag coefficient at each wing section is calculated from the experimentally obtained drag polar for the given airfoil section.

2.1.3 Aeroelastic Analysis

The aeroelastic analysis of this high-aspect-ratio wing is based on the assumption that the aerodynamic forces due to twist can be adequately modeled in terms of the twist angles of n_c selected chords of the wing and integrated to provide point loads

at the aerodynamic centers of these chords, where n_c is equal to 8 in the present study.

The structural model has n_{dof} degrees of freedom, and the load vector F of order n_{dof} depends on the angle of attack α and the vector of elastic twist angles θ (of order n_c). So,

$$F = F_e + E(\alpha qR + q\bar{A}\theta) \tag{1}$$

where F_e is the force vector of order n_{dof} on the undeformed structure at zero angle of attack, R is the incremental force vector of order n_c per unit angle of attack at the aerodynamic center, q is the dynamic pressure, $\bar{A}$ is a n_c by n_c aerodynamic influence coefficient matrix such that $q\bar{A}_{ij}$ represents the change in lift force in chord i due to a unit twist angle at chord j. The elements of the R vector are the sum of the corresponding rows of $\bar{A}$. The transformation matrix E (of order n_{dof} by n_c) transforms force vectors from the aerodynamic centers to the structural grid points.

The twist vector θ due to F is given as

$$\theta = S(\alpha qR + q\bar{A}\theta) + TK^{-1}F_e \tag{2}$$

where S is a reduced flexibility matrix relating forces at the aerodynamic centers of the n_c chords to the twist angles at those chords. The matrix T relates displacements at the structural grid to twist angles, and K is the structural stiffness matrix. To calculate the flexibility matrix, we start by generating a unit load matrix U (of order n_{dof} by n_c) with each column corresponding to a unit load applied at one aerodynamic center. The displacement matrix due to U is found from the equations of equilibrium

$$KQ = U \tag{3}$$

Finally, the twist angles corresponding to the elements of S are calculated as

$$S = TQ \tag{4}$$

We also have a requirement that the total force on a wing is equal to half the weight W of the aircraft times the load factor n

$$N^T E(\alpha qR + q\bar{A}\theta) + N^T F_e = \frac{1}{2} nW \tag{5}$$

where N is a vector of order n_{dof} with all components in the z direction equal to 1. Using Eq. (5) , we get

$$\alpha = \frac{(0.5nW - qN^T E\bar{A}\theta - N^T F_e)}{qN^T ER} \tag{6}$$

Substituting back into Eq. (2), we have

$$\theta = S(\beta qR + qA^{\times}\theta) + TK^{-1}F_e \tag{7}$$

where

$$A^{\times} = \bar{A} - \frac{(RN^T E\bar{A})}{N^T ER} \tag{8}$$

and

$$\beta = \frac{(0.5nW - N^T F_e)}{qN^T ER} \tag{9}$$

Finally from Eq.(7), we get

$$(I - qSA^{x})\theta = \beta qSR + TK^{-1}F_e \tag{10}$$

where I is the unit matrix. θ is now calculated by solving Eq(10), and θ, α are then used to obtain a lift distribution C_l as

$$C_l = C_{lb} + \alpha R + A\theta \tag{11}$$

where C_{lb} is a based lift distribution from an aerodynamic analysis.

The divergence dynamic pressure is obtained by solving the eigenvalue equation

$$(I - qS\bar{A})\theta = 0 \tag{12}$$

with the lowest eigenvalue corresponding to the divergence dynamic pressure, q_d.

The reason for using $\bar{A}$ instead of A^x in the equation (12) is that the latter includes the effect of a pilot correction to angle of attack to keep the lift force be constant. During divergence, the pilot has no time to apply this correction. Fig. 5 shows a typical plot of loads at the aerodynamic centers for the rigid and elastic wing. The corresponding elastic twist and average displacement at the tip are 5.44 degree and 0.10 m, respectively.

2.2 Efficient Cross-Sensitivity Derivatives

From the above aeroelastic analysis, two cross-sensitivity matrices, which are the aerodynamic influence coefficient matrix A and the flexibility matrix S, characterize

the interaction between aerodynamics and structure. For n_c selected chords, the calculations of these matrices required calling n_c executions of the vortex-lattice program and n_c executions of the finite-element program for a single analysis, and this accounted for major cost of the aeroelastic analysis. A typical aeroelastic design problem may need thousands such analyses in a design cycle to get aeroelastic sensitivities such as derivatives of the θ with respect to design variables. Traditionally, they are obtained by a finite difference method that requires the recalculation of A and S for perturbed designs which is expensive in the design optimization. One way to alleviate the cost for repeated calculations of A and S is to use a linear Taylor series approximation for each matrix, that is

$$A = A_0 + \sum_{i=1}^{NDV} \frac{\partial A}{\partial x_i} \Delta x_i \tag{13}$$

$$S = S_0 + \sum_{i=1}^{NDV} \frac{\partial S}{\partial x_i} \Delta x_i \tag{14}$$

where NDV is a number of design variables. The computational costs will then depend on the efficiency of calculating the derivatives of A and S matrices. The following two sections discuss their calculations using a perturbation method for the aerodynamic sensitivity and an adjoint method for the flexibility sensitivity.

2.2.1 Efficient Calculation of the Aerodynamic Matrix

The matrix A is found for a given wing planform and twist distribution using the VLM and unit displacement states by finite differences. First, the base lift distribution is determined by a VLM analysis for some median angle-of-attack. Next, a unit rotation is imposed at the first wing section and a new lift distribution is found from second VLM analysis. The difference between the new lift coefficients and the base loft coefficients at each of the stations forms the first column in the A matrix. The other columns are found in a similar manner.

In order to reduce the costs associated with the A matrix computation, a perturbation form of the vortex lattice method was developed in Ref(19). Table 1 gives the computational time on IBM 3090 for the A matrix using finite differences and one using the perturbation approach for 80, 120, 160 and 200 panels.

2.2.2 Derivatives of the Flexibility Matrix

To calculate $\partial S/\partial x$, where x is a structural sizing design variable, such as a skin thickness, we differentiate Eq.(3) and (4), and get the following equations.

$$K\frac{\partial Q}{\partial x} = -\frac{\partial K}{\partial x}Q \tag{15}$$

$$\frac{\partial S}{\partial x} = T\frac{\partial Q}{\partial x} \tag{16}$$

Notice that T is only a function of the geometry design variables but not of the structural sizing variables.

The so called direct way to calculate $\partial S/\partial x$ is to solve Eq.(15) for $\partial Q/\partial x$ and substitute it into Eq.(16). With this approach, Eq.(15) needs to be solved once for each structural sizing variable, and since Q is a matrix with n_c columns, this is equivalent to a solution for n_c load vectors for each design variable. It is relatively expensive when we have a large number of design variables.

Instead we developed an adjoint method. We first define an adjoint matrix B obtained from the solution of

$$KB = T^T \tag{17}$$

Combining equations (15), (16), and (17), we get

$$\frac{\partial S}{\partial x} = -B^T\frac{\partial K}{\partial x}Q \tag{18}$$

The main computational effort is Eq.(17) which requires the solution for n_c load vectors (the columns of T^T) and is independent of the number of design variables. The adjoint approach is therefore a much more efficient way for calculating derivatives of the flexibility matrix than the direct approach.

The derivatives of S with respect to the structural variables, obtained as above, are supplemented by finite-difference derivatives with respect to the four geometric planform design variables. Then the flexibility matrix is approximated linearly as shown in Eq(14).

Table 2 shows CPU seconds on IBM 3090 for the finite-difference calculation of the derivatives of lift distribution using two different approaches to get the S matrix. In the first row an exact S is used, it requires a total 78.6 seconds which include 47.4 seconds to generate the S matrix and 31.2 seconds to perform aerodynamic analyses. In the second row an approximated S is used, it requires a total 41.5 seconds which include 10.3 seconds to calculate the derivatives of the S matrix and 31.2 seconds to perform aerodynamic analysis. Overall, the CPU cost is reduced to 41.5 CPU seconds, a reduction of 47.2%.

2.3 Design Optimization

2.3.1 Sailplane Wing Design Problem

The mission profile for the sailplane involves climbing to a height H in a prescribed thermal, then cruising a distance D while losing the altitude H, as depicted in Fig. 6. The objective function is the cross-country speed of the glider which is the average speed considering both phases of the flight.

Two design procedures are compared. The first procedure is an iterated, sequential design procedure. The aerodynamic design is obtained for an initial estimate of the weight by varying the aerodynamic variables to maximize the cross country speed. The loads based on this aerodynamic design are then used to optimize the structure for minimum weight, and the new weight is used to restart the aerodynamic design. The process is continued until the weight is converged. The second procedure is an integrated design procedure that combines both the aerodynamic and structural design together. One integrated design procedure maximizes the cross-country speed. Another integrated design procedure minimizes the structural weight subject to an additional constraint that the cross-country speed should be at least 2.80 m/sec (the value obtained from the iterated, sequential design procedure).

The structure is designed to carry the loads associated with a 5.9g pull-up maneuver. Maximum strain constraints ($\varepsilon_1 < 0.004$, $\varepsilon_2 < 0.004$, $\varepsilon_{12} < 0.004$) were imposed on each composite lamina. For the spar caps, the strain is limited to 0.003. Maximum shear

stress of 34.0 MPa is used for the spar webs. The divergence dynamic pressure is greater than 1.2 times the dynamic pressure at 5.9g maneuver.

The design variables and constraints used in the present study are summarized in Table 3 and 4.

2.3.2 Approximate Optimization Procedure

In large-scale design optimization problems, most of the computational cost stems from repetitive execution of analysis program. The costs can be reduced by using approximate analysis method which replaces the more expensive full analysis. A sequential approximate optimization algorithm is considered to be the best approach (Ref. 22). This approach replaces the original objective function and constraints with approximations based upon nominal values and derivatives at an initial point. Move limits are used to prevent the design from moving outside the bound of validity of the approximations. After an optimum is found, a new approximation is constructed there, and the process repeated until convergence is achieved.

When we first attempted to use sequential approximate optimization for the combined structural/aerodynamic design problem, convergence was found to require extremely tight move limits of one or two percent change in design variables. The problem was

traced to the objective function, the average cross-country speed of the glider V_c , which cannot be adequately represented by a linear approximation near the optimum where it has high curvature. This problem was solved by using a linear approximation to the lift coefficient distribution on the wing and calculating the performance exactly from the approximate lift distribution. Fig. 7 compares the exact objective function, the linear approximation to the objective function and the approximation based upon the linearized lift distribution. It is seen that the approximation based upon the linearized lift is almost identical to the exact objective function. This good approximation permits larger changes in design variables at each approximate optimization.

For the sailplane design study, the optimization problem can be formulated as:

$$\begin{aligned} &\text{Maximize} && V_c(x_a, x_s) \\ &\text{such that} && g_a(x_a, x_s) \geq 0 \\ &\text{and} && g_s(x_a, x_s) \geq 0 \end{aligned} \tag{19}$$

where the vector g_a represents the aerodynamic constraints, such as limits on bank angle and stall, and g_s represent structural constraints on stresses, strains and aeroelastic stability. Each approximate optimization problem starting from an initial design x_a^0 , x_s^0 is formulated as:

$$
\begin{aligned}
&\text{Maximize} \quad V_c(x_a, C_l) \\
&\text{such that} \quad g_a(x_a^0, x_s^0) + \sum_i^{NDV} \frac{\partial g_a}{\partial x_i}(x_i - x_i^0) \geq 0 \\
&\text{and} \quad g_s(x_a^0, x_s^0) + \sum_i^{NDV} \frac{\partial g_s}{\partial x_i}(x_i - x_i^0) \geq 0 \\
&\text{where} \quad C_l = C_l(x_a^0, x_s^0) + \sum_i^{NDV} \frac{\partial C_l}{\partial x_i}(x_i - x_i^0)
\end{aligned}
\tag{20}
$$

2.3.3 Design Program

The wing design program includes five main modules which are a design variable module, an aerodynamic module, a flexibility module, an aeroelastic module and an optimization module. The design variable module initially defines all parameters and design variables. After each design optimization, new design variables replace these initial values. The aerodynamic module generates a base aerodynamic matrix, A^0 and derivatives of the aerodynamic matrix with respect to 6 planform design variables. The flexibility module gives a base flexibility matrix, S^0 and derivatives of the flexibility matrix with respect to 32 structural sizing design variables and 4 shape design variables. The aeroelastic module calculates base lift distributions, C_l aerodynamic constraints, g_a, structural constraints, g_s as well as their sensitivities at 5.9g pull-up maneuver. The optimization module performs the design optimization. The

optimizer is the NEWSUMT-A program (Ref. 23) which is based on an extended interior penalty procedure, and allows for various levels of constraint and objective function approximations. Fig. 8 shows a flow chart of the flexibility module. Fig. 9 shows a flow chart of the aeroelastic module.

2.3.4 Optimization Results

An attempt to perform a design without using the cost-reducing procedures discussed above proved infeasible. Based on a single one-dimensional optimization the computational requirement were estimated at about 5 hours of IBM 3090 CPU time. Using the approximate procedures discussed here, the complete design process required 4 overall design cycles of 94 CPU seconds each for a total time of 376 CPU seconds. Approximately 40% of the CPU time was needed to calculate the A matrix sensitivity, 11% to calculate the S matrix sensitivity, 34% to determine the lift and constraint sensitivity by using the linear Taylor series approximation of the A and S matrix, and 15% for the optimization itself.

The results of the integrated design procedure for the sailplane wing are summarized in Table 5. In the first column of this table are the results for the iterated, sequential design procedure. The second column of the table corresponds to the integrated aerodynamic-structural design which optimized the cross-country speed, the third

column of the table refers to a weight minimization integrated design. In comparing the three designs, the general trends are similar those obtained with more rudimentary analysis methods in Ref. 15. We see that the increase in performance of the integrated design as compared to the iterated, sequential design was 1% with as 7% reduction in weight. Also, the same performance as the iterated, sequential design could be achieved through an integrated design with nearly 16% less weight.

This investigation of the design process of a composite sailplane wing, reconfirms the conclusions of the previous work, Ref. 15, in demonstrating the superiority of an integrated design approach over an iterative, sequential procedure. The integrated design was able to capitalize on favorable interactions between aerodynamics and the structure. These interactions included distributing the structural material so deformations did not reduce aerodynamic performance, and reducing the weight of the wing to increase the overall performance. Wing structural weight was reduced by concentrating more of the lift inboard and by reducing the planform area of the wing, resulting in lower root bending moments. The reduced weight was accompanied by reduced torsional stiffness and greater deformations. The separation of the two disciplines in the iterative procedure did not allow such interactions to be taken into account and applied towards improvement of the design.

Chapter 3

Forward-Swept Subsonic Transport Wing Design

The subsonic transport wing design represents our next goal to efficiently integrate aerodynamic and structural wing design. Unlike the integrated sailplane design, we use more refined models for the aeroelastic analysis. For example, the aerodynamic forces in the sailplane wing design have been lumped at only 8 points along the wing span (one point per chord), while we lump the aerodynamic forces at several points along each chord for a total of 48 points in the transport wing design. With this change, the size of the A matrix and the S matrix needed in the aeroelastic analysis will both increase from an 8 by 8 matrix to a 48 by 48 matrix. Although we have developed efficient sensitivity calculations of these two matrices in the sailplane design, to deal with a larger problem, we anticipated the need for further computational savings. This was achieved by using a modular sensitivity method (Refs. 17,18). With this method, aeroelastic sensitivities can be computed without the expensive calculation of the derivatives of the A and S matrices which are needed in the sailplane

design. Other differences between the current and the previous design problem are the objective function, the constraints, the design variables and wing configurations.

3.1 Analysis

3.1.1 Structural Model

The finite element model of the forward-swept transport wing is shown in Fig. 10. Because of the complexity of the wing a finite-element mesh generator was developed. The mesh generator first determines coordinates at the root, break and tip from six shape design variables. The nodal coordinates are then calculated and based on parameters such as number of spar caps, rib angles measured from a front spar, and rib spacing measured normal to the rib. The model has 534 degrees of freedom and 1093 elements. There are 684 anisotropic triangular membrane elements to model the graphite/epoxy wing skins which were again stacked up of 0^0, $\pm 45^0$ and 90^0 plies. There is a ply orientation design variable which corresponds to rotating all plies with the same angle. A total of 133 shear web elements model the spar webs. The remaining elements are truss elements which model the spar caps, model the vertical stiffness of ribs and spars, and provide a crude model of the leading/trailing edge structure. The leading and trailing edge truss elements are used for the purpose of transferring aerodynamic loads to the wing box. The material properties of the graphite/epoxy are E1 = 131.0 GPa, E2 = 13.0 GPa, ν_{12} = 0.38 and G12 = 6.4 GPa.

3.1.2 Aerodynamic Model

The planform of the forward-swept transport wing is shown schematically in Fig. 11. The six parameters x_1 - x_6 represent planform design variables. Two other aerodynamic design variables are the twist angles at the break and the tip. The airfoil section, for all spanwise stations is the HSNLF(1)-0213, described in Ref. 24. The aerodynamic analysis is still based on a vortex-lattice method (VLM). In this approach, the continuous distribution of bound vorticity over the wing surface is approximated by a finite number of discrete horseshoe vortices that are placed in trapezoidal panels. For the transport design we used a total number of 120 panels, (12 spanwise, 10 chordwise) to model the wing. The lift and induced drag are computed from the integrated circulation distribution. The profile drag coefficient at each wing section is calculated from the experimentally obtained drag polar for the given airfoil section.

3.1.3 Aeroelastic Analysis

The aeroelastic analysis differs from the one used in the sailplane design. The major difference is the aerodynamic forces in the previous aeroelastic analysis were assumed to be a linear function of the angle of attack and structural deformations. This assumption allows us to solve those aeroelastic equations analytically. In general, these forces are nonlinear functions of the angle of attack and structural deformations so that the aeroelastic analysis results in a set of nonlinear aeroelastic equations solved by Newton's method. Additionally, the structural deformation vector θ included 8 twist angles in the sailplane wing design and 48 vertical displacements in the forward-swept wing design. Due to this change, the A and S matrices have different physical meanings.

The aeroelastic analysis of the forward-swept transport wing is simplified by making several assumptions. We assume that the effect of the aerodynamics on structural deformations can be approximated by lumping the aerodynamic forces at n_l structural grid points (called here the load set), and including only the vertical components of the loads. In the present study, n_l is equal to 48. The vector of vertical aerodynamic loads is denoted as F_a. We assume that the overall aircraft response affects the wing only through the root angle of attack α. Finally, we assume that the effect of structural deformations on the aerodynamic response can be approximated in terms of the vector of vertical displacements θ at the load set.

The formulation of the aeroelastic analysis is based on a system approach; that is, the behavior of the system is described by a set of coupled subsystem equations (Ref. 17). Each of the subsystem equation represents a particular engineering discipline

or a distinct physical part of the system. In our case, we have an aerodynamic subsystem, a performance subsystem and a structural subsystem.

The aerodynamic subsystem analysis generates the vertical aerodynamic loads, F_a, at the load set. It is described by a functional relationship as

$$F_a = q\, f_1(p, \alpha, \theta) \tag{21}$$

where q is the dynamic pressure, and p is a vector of design parameters.

The performance subsystem is characterized by only the root angle of attack, α. It is obtained from the overall equilibrium of the aircraft as

$$f_2(p, F_a) = \frac{1}{2} nW_G - N^T F_a = 0 \tag{22}$$

where N is a summation vector, n is the load factor and W_G is the gross weight of the transport aircraft, and will be defined in detail later on.

The structural subsystem analysis gives the vertical displacements at the load set. We first obtain a nodal displacement vector U by solving

$$KU = TF_a + nF_l \tag{23}$$

where K is the stiffness matrix, T is a Boolean matrix which expands F_a to the full set of structural degrees of freedom, and F_l is the gravitational and inertia load vector. The vertical displacements at the load set θ are then extracted from U as

$$\theta = T^T U \tag{24}$$

Equations (23) and (24) can be combined as

$$\theta = f_3(p, F_a) \tag{25}$$

Mathematically, the three subsystem equations represent a set of nonlinear coupled equations for the vector of vertical aerodynamic loads F_a , the wing root angle of attack, α and the the vertical displacements θ. To solve these equations, we use Newton's method with an initial estimate for the solution F_a^0 , α^0 , θ^0 . Then, the first iteration with Newton's method generates a system of linear equations as

$$J\Delta Y = \Delta f \tag{26}$$

where ΔY, Δf and J are defined below in equations (27), (28) and (29).

$$\Delta Y = \{\Delta F_a, \Delta\alpha, \Delta\theta\}^T \tag{27}$$

$$\Delta f = \begin{Bmatrix} q\, f_1(p, \alpha^0, \theta^0) - F_a^0 \\ f_2(p, F_a^0) \\ f_3(p, F_a^0) - \theta^0 \end{Bmatrix} = \begin{Bmatrix} \Delta f_1 \\ \Delta f_2 \\ \Delta f_3 \end{Bmatrix} \tag{28}$$

$$J = \begin{bmatrix} I & -q\partial f_1/\partial\alpha & -q\partial f_1/\partial\theta \\ -\partial f_2/\partial F_a & 0 & 0 \\ -\partial f_3/\partial F_a & 0 & I \end{bmatrix} = \begin{bmatrix} I & -qR & -qA \\ N^T & 0 & 0 \\ -S & 0 & I \end{bmatrix} \tag{29}$$

The Jacobian J is given in terms of the dynamic pressure q, the incremental aerodynamic force vector, qR, the aerodynamic influence coefficient matrix, qA and the

flexibility matrix S. The incremental aerodynamic force vector is defined such that its component q r_i represents the change in F_{ai} due to a unit change in α, and the aerodynamic influence coefficient matrix is defined such that its component qa_{ij} represent the change in F_{ai} due to unit change in θ_j . Similarly, the flexibility matrix S, is such that s_{ij} is the change in θ_i due to a unit change in F_{ai} .

Partial solution of equation (26) yield the following three system analysis equations for the increments $\Delta\theta$, $\Delta\alpha$, ΔF_a :

$$(I - qSA^{x})\Delta\theta = SB\Delta f_1 + \frac{SR}{N^T R}\Delta f_2 + \Delta f_3 \tag{30}$$

$$\Delta\alpha = \frac{\Delta f_2 - N^T\Delta f_1 - qN^T A\Delta\theta}{qN^T R} \tag{31}$$

$$\Delta F_a = \Delta f_1 + qR\Delta\alpha + qA\Delta\theta \tag{32}$$

where we define

$$B = I - \frac{RN^T}{N^T R} \tag{33}$$

and

$$A^{\times} = BA \tag{34}$$

In our case we start with a rigid wing approximation $F_a^0 = F_{ar}$, $\alpha^0 = \alpha_r$, $\theta^0 = 0$, where

$$F_{ar} = q\, f_1(p,0,0) + q\alpha_r R \tag{35}$$

At cruise (n = 1), we have $q = q_c$

$$\alpha_r = \frac{0.5W_G - N^T q_c f_1(p,0,0)}{q_c N^T R} \tag{36}$$

By Eq.(28), we get

$$\Delta f = \begin{Bmatrix} q_c f_1(p, \alpha_r, 0) - F_{ar} \\ 0 \\ f_3(p, F_{ar}) \end{Bmatrix} \tag{37}$$

At 2.5g maneuver (n = 2.5), the initial conditions for the wing become $F_a^0 = \bar{F}_{ar}$, $\alpha^0 = \bar{\alpha}_r$, $\theta^0 = 0$, where $q = q_m$ ($q_m = 2.5q_c$), where

$$\bar{F}_{ar} = q_m f_1(p,0,0) + q_m \bar{\alpha}_r R \tag{38}$$

$$\bar{\alpha}_r = \frac{1.25W_G - q_m N^T f_1(p,0,0)}{q_m N^T R} \tag{39}$$

The corresponding $\Delta\bar{f}$ of Eq.(28) is

$$\Delta\bar{f} = \begin{Bmatrix} q_m f_1(p, \bar{\alpha}_r, 0) - \bar{F}_{ar} \\ 0 \\ f_3(p, \bar{F}_{ar}) \end{Bmatrix} \tag{40}$$

In each aeroelastic analysis, a single Newton iteration is used to approximate the flexible wing response.

The aeroelastic divergence instability is calculated at a fixed angle of attack, because it is assumed that the pilot does not react fast enough to change the angle of attack as the wing diverges. The instability is characterized by a homogeneous solution to Eq.(26), that is

$$\begin{bmatrix} I & -qA \\ -S & I \end{bmatrix} \begin{Bmatrix} \Delta F_a \\ \Delta\theta \end{Bmatrix} = 0 \tag{41}$$

Equation (41) is an eigenvalue problem for q. We denote the corresponding eigenvector as $[F_{aD}, \theta_D]^T$. Equation (41) can be reduced to a standard eigenvalue problem by substituting for $\Delta\theta$ in terms of ΔF_a . That is

$$\Delta\theta = S\Delta F_a \tag{42}$$

and obtain

$$(AS - \frac{1}{q} I)\Delta F_a = 0 \tag{43}$$

with the lowest real eigenvalue corresponding to the divergence dynamic pressure, q_D at 2.5g maneuver.

Fig. 12 shows a typical plot for the rigid and elastic loads, showing a favorable bending-twisting coupling that bending causes a nose-down twist. This was achieved by orienting the zero direction of the composite skins towards the free stream velocity. Fig. 13 shows an opposite result obtained by orienting the zero direction away from the free stream velocity which results in a nose-up twist due to bending. The divergence speed of the first example is 1110 m/sec, whereas in the second example, it is reduced to 226 m/sec.

3.2 Modular Sensitivity Analysis

3.2.1 Aeroelastic Sensitivities

The modular sensitivity approach avoids the expensive calculations of the derivatives of the aerodynamic influence coefficient matrix A′ and the derivatives of the flexibility matrix S′ . First, we differentiate the subsystem equations (21), (22) and (25) with respect to a design variable p to obtain

$$\frac{\partial F_a}{\partial p} = q\frac{\partial f_1}{\partial p} + q\frac{\partial f_1}{\partial \alpha}\frac{\partial \alpha}{\partial p} + q\frac{\partial f_1}{\partial \theta}\frac{\partial \theta}{\partial p} \tag{44}$$

$$\frac{\partial f_2}{\partial p} + \frac{\partial f_2}{\partial F_a}\frac{\partial F_a}{\partial p} = 0 \tag{45}$$

$$\frac{\partial \theta}{\partial p} = \frac{\partial f_3}{\partial p} + \frac{\partial f_3}{\partial F_a}\frac{\partial F_a}{\partial p} \tag{46}$$

These equations can be rearranged and expressed in a matrix form as

$$JY' = f' \tag{47}$$

where a prime denotes differentiation with respect to p and where

$$Y' = [F_a', \alpha', \theta']^T \tag{48}$$

and

$$f' = [qf_1', f_2', f_3']^T \tag{49}$$

along with the definition $f_i' = \partial f_i / \partial p$ for i = 1, 2, 3. The Jacobian J appearing in Eq.(47) is the identical matrix utilized in the analysis equation (26). Then, Eq.(47) can be partially solved to yield

$$(I - qSA^x)\theta' = SBqf_1' + \frac{SR}{N^T R} f_2' + f_3' \tag{50}$$

$$\alpha' = \frac{f_2' - qN^T f_1' - qN^T A\theta'}{qN^T R} \tag{51}$$

$$F_a' = qf_1' + qR\alpha' + qA\theta' \tag{52}$$

The alternate approach which is to perturb the system analysis equations (30), (31), and (32) inevitably require the derivatives of A and S. The modular approach does not require any derivatives of A and S but only partial derivatives of f_1 , f_2 , and f_3 .

For example, f_3' denotes the derivative of θ with respect to a design variable when F_a and α are fixed.

To illustrate for a structural parameter, the three partial derivatives are

$$f_1' = 0 \tag{53}$$

$$f_2' = \frac{1}{2} n W_G' \tag{54}$$

$$f_3' = (T^T K^{-1} T)' F_a + n T^T (K^{-1} F_l)' \tag{55}$$

Our procedure obtains f_2' and f_3' by a forward finite-difference method. Table 6 compares the θ sensitivities with respect to a skin thickness near the wing root using both the modular approach and an overall finite-difference approach where the entire analysis is repeated for a perturbed design variables. In terms of time saving, for one structural sizing design variable, the modular approach spends about 6.53 CPU seconds on IBM 3090 compared with 9.59 CPU seconds for the direct approach, a 32% saving in CPU time.

After we calculate the derivatives of the aeroelastic response we can calculate derivatives of the total drag of the aircraft with respect to p, $\partial D/\partial p$. For an elastic wing, we can express the drag as a function of p, α and θ as

$$D = f_4(p,\alpha,\theta) \tag{56}$$

Taking the derivative of above equation, we get

$$\frac{\partial D}{\partial p} = \frac{\partial f_4}{\partial p} + \frac{\partial f_4}{\partial \alpha}\frac{\partial \alpha}{\partial p} + \frac{\partial f_4}{\partial \theta}\frac{\partial \theta}{\partial p} \tag{57}$$

where $\partial f_4/\partial p$ is the derivatives of the drag at a fixed angle of attack and fixed structural deformation.

3.2.2 Divergence Sensitivities

To find the derivative of the divergence dynamic pressure q_D with respect to a design parameter p, we differentiate Eq.(41) at $q = q_D$ with respect to p

$$\begin{bmatrix} 1 & -q_D A \\ -S & 1 \end{bmatrix} \begin{Bmatrix} F_{aD}' \\ \theta_D' \end{Bmatrix} + \begin{bmatrix} 1 & -(q_D A)' \\ -S' & 1 \end{bmatrix} \begin{Bmatrix} F_{aD} \\ \theta_D \end{Bmatrix} = 0 \tag{58}$$

We premultiply Eq.(58) by the left eigenvector of Eq.(41), $[F_{aL}, \theta_L]^T$, defined by

$$\left[F_{aL}^T, \theta_L^T\right]\begin{bmatrix} I & -(q_D A) \\ -S & I \end{bmatrix} = 0 \tag{59}$$

and obtain

$$\left[F_{aL}^T, \theta_L^T\right]\begin{bmatrix} I & -(q_D A)' \\ -S' & I \end{bmatrix}\begin{Bmatrix} F_{aD} \\ \theta_D \end{Bmatrix} = 0 \tag{60}$$

or

$$q_D{}' = -\frac{q_D F_{aL}^T A' \theta_D + \theta_L^T S' F_{aD}}{F_{aL}^T A \theta_D} \tag{61}$$

To compute the left eigenvectors, Eq.(59) is reduced to a standard eigenvalue problem by substituting for θ_L in terms of F_{aL} as

$$F_{aL}^T = \theta_L^T S \tag{62}$$

and obtain

$$\left[(SA)^T - \frac{1}{q} I\right]\theta_L = 0 \tag{63}$$

Equation (61) contains derivatives of A and S with respect to p which we have managed to avoid before. However, the corresponding terms can be simplified. Using the definition of S, Eq.(29), we note that

$$S'F_{aD} = \frac{\partial}{\partial p}\left(\frac{\partial f_3}{\partial F_a}\right)F_{aD} \tag{64}$$

To see how $S'F_{aD}$ can be calculated without obtaining S' we consider a more generic case. Let f be a function of a vector X, and let D be another vector. Let X_0 be a particular choice for X, then

$$\frac{\partial f}{\partial X}(X_0)D = \lim_{\varepsilon \to 0} \frac{1}{\varepsilon}[f(X_0 + \varepsilon D) - f(X_0)] = \frac{d}{d\varepsilon} f(X_0 + \varepsilon D) \simeq \frac{f(X_0 + \varepsilon D) - f(X_0)}{\varepsilon} \tag{65}$$

Equation (65) provides us with a way of calculating the product $\frac{\partial f}{\partial X}(X_0)D$ without calculation the individual components of $\partial f/\partial X$. Therefore, to calculate $S'F_{aD}$ we start

by calculating the derivative of f_3 to a perturbation in F_a in the form of F_{aD} (because we use linear structural analysis this is the response of the structural to F_{aD}). Then we calculate the derivative of this response with respect to p assuming that F_{aD} is fixed. The term $A'\theta_D$ in Eq.(61) is treated in a similar way.

For a structural design variable which is the skin thickness near the wing root, a typical value of the q_D' by the modular approach is like -3.0295638 x 10^4 N/m^3. This value was compared with an overall finite-difference approach which gives us q_D' to be equal to -3.0306667 x 10^4 N/m^3.

3.3 Design Optimization

3.3.1 Forward-Swept Wing Design Problem

We are considering the design of a forward-swept composite wing for a subsonic transport aircraft. The goal is to reduce the gross weight of the aircraft. This is achieved by minimizing the weight of the wing which in turn allows a reduction in weight of other structural components. The saving in the weight can be used to reduce the cost of the aircraft, to increase its range or to increase the payload. Many of the design specifications are taken from a reference aircraft summarized in Table

7. We replace the backward-swept wing of the reference aircraft with a forward-swept wing which is based on a study of laminar flow aircraft design concepts (Ref. 25), and we reduce the cruise Mach number from 0.78 to 0.48.

The objective function to be minimized for the design is the gross weight of the aircraft, W_G which is defined as

$$W_G = W_S + W_{UF} + W_P \tag{66}$$

where W_S is the aircraft standard empty weight, W_{UF} is an usable fuel weight and W_P is a payload weight. In Eq.(66), the usable fuel weight is a design variable which affects both the gross weight and the range calculation.

The standard empty weight of the design aircraft, W_S, is calculated from that of the reference aircraft by assuming that structural weight saving in the wing is amplified by a factor η due to saving on non-structural weight in wing and savings in fuselage, tail and power plant. Then we have

$$W_S = W_{RS} - (W_{RW} - W_W)\eta \tag{67}$$

where W_{RS} is a standard empty weight of the reference aircraft, W_{RW} is a structural wing weight of the reference aircraft, W_W is a structural wing weight of the design aircraft, and η is a structural weight gain amplification factor. The variable η is assumed to be 2. This implies that for every Newton of weight saved in the wing weight,

one additional Newton is saved in non-structural weight and in other structural components.

The structural wing weight depends on structural design variables and the planform parameters. The structural design variables include panel thicknesses, spar cap areas and ply orientation. The aerodynamic design variables are the planform shape parameters and the twist schedules along the span. The twist schedules roughly represent the jig shapes of the transport wing.

The cruise dynamic pressure is also a design variable. The dynamic pressure depends on both air density and air velocity. In our design procedure, we assume a constant cruise speed, so the dynamic pressure defines air density, and hence the cruise altitude. In other words, an optimum cruise altitude will be indirectly found by the optimizer at the end of the design.

The structure is designed to withstand a 2.5g pull-up maneuver with a 1.5 factor of safety. The maneuver is assumed to follow an altitude loss and occurs at 2.5 times the cruise dynamic pressure. Maximum strain constraints ($\varepsilon_1 < 0.012$, $\varepsilon_2 < 0.012$, $\varepsilon_{12} < 0.012$) were imposed on each composite lamina. We have 228 such constraints for the 0^0, $\pm 45^0$, and 90^0 plies belonging to the upper and lower skins. Maximum stress 2.62×10^8 MPa is used for the spar caps. The aeroelastic constraint is formulated as the divergence dynamic pressure to be greater than 1.2 times the dynamic pressure at the 2.5g maneuver.

There are two performance constraints. One is a range constraint requiring the design to at least have the same range as the reference aircraft. The second constraint is a volume constraint that ensures we have enough space inside the wing to carry

the necessary fuel during the flight. Details about performance calculations can be found in the Appendix. Table 8 and Table 9 summarize the design variables and constraints.

3.3.2 Approximate Optimization Procedure

For the transport aircraft design, the optimization can be formulated as

$$\begin{aligned} &\text{Minimize} && W_G(p) \\ &\text{such that} && g_s(p) \geq 0 \\ & && V_s(p) \geq V_r \\ & && R_g(p,D) \geq R_r \end{aligned} \tag{68}$$

where the vector g_s represent structural constraints on stresses, strains and aeroelastic stability. V_s and V_r are the available wing volume, and the required fuel volume, respectively. R_g is the calculated range which depends on the total drag D of the aircraft and is greater than the range of the reference aircraft which is 2.34 x 10^6 m or 1.45 x 10^3 miles.

Even with the more efficient sensitivity analysis, a fully coupled structural-aerodynamic analysis and sensitivity is quite expensive. Thus, we still use the sequential approximation optimization algorithm with move limits as in the sailplane design. The range constraint is calculated exactly from a linear approximation to the

drag. Each approximate optimization problem starting from an initial design p^0 is formulated as:

$$\begin{aligned}
&\text{Minimize} \quad W_G(p) \\
&\text{such that} \quad g_s(p^0) + \sum_i^{NDV} \frac{\partial g_s}{\partial p_i} \Delta p_i \geq 0 \\
&\qquad\qquad V_s(p) \geq V_r \\
&\qquad\qquad R_g(p,D) \geq R_r \\
&\text{where} \quad D = D(p^0) + \sum_i^{NDV} \frac{\partial D}{\partial p_i} \Delta p_i
\end{aligned} \tag{69}$$

The exact drag and the linear approximation to the drag are compared in Fig. (14).

3.3.3 Design Program

The design procedure is shown schematically in Fig. 15. First, the initialization module initializes and changes the design variables as well as defines all parameters. Next, the wing geometry and load sets are determined to start with a structural analysis for the S matrix, and an aerodynamic analysis for the A matrix and R vector. We then perform an aeroelastic/sensitivity analysis to get the drag sensitivities at the

cruise, and the stress, strain and divergence sensitivities at the maneuver. The details of these analyses will be shown later on. Finally, the optimization module optimizes the design using the sensitivity information calculated before. After an optimum is found, a new approximation is constructed there, and the process is repeated until convergence is achieved.

Fig. 16 shows a flow chart for the aeroelastic sensitivity calculation at cruise. The aeroelastic analysis first gives the F_a , α and θ which are used to calculate functions of f_1 , f_2 , and f_3 . We then compute the partial derivatives of f_1 , f_2 , and f_3 with respect to design variables by a forward finite difference method. Solving the modular sensitivity equations to obtain F_a', α', θ' , we finally get the drag sensitivity from Eq. (57).

Fig. 17 shows a flow chart for the structural sensitivity calculation. The dynamic pressure at 2.5g maneuver is greater than the dynamic pressure at the cruise. We thus require to perform another aeroelastic analysis. After solving the right and left eigenvalue problems, we then get the divergence dynamic pressure and the associated eigenvectors which are used to calculate $S'F_{aD}$ and $A'\theta_D$. Next, we perform the modular sensitivity analysis as before. To get the stress and strain sensitivity by an overall finite difference approach, we need the new aerodynamic loads F_a due to perturbations of the design variables. Calculating the perturbed aerodynamic loads by an exact aeroelastic analysis is relatively expensive. Instead we use a linear Taylor series approximation to F_a where the F_a' is obtained from the modular sensitivity analysis.

3.3.4 CPU Time Comparison

The CPU time (IBM 3090) used to generate the flexibility matrix (of order 48 by 48) is 4.91 seconds, and to generate the aerodynamic influence coefficient matrix (of order 48 by 48) is 224.54 seconds. The total CPU time for one design cycle is about 797 seconds. Approximately 31% of the CPU time is needed to calculate the A matrix, 1% to calculate the S matrix, 21% to determine the drag sensitivities, 46% to determine the structural sensitivities, and only 1% for the optimization itself.

To calculate the aeroelastic sensitivities such as F_a', α', θ' and q_D' by a finite-difference method, in our design problem, we need to calculate the A matrix 9 more times for 9 aerodynamic design variables, and the S matrix 35 more times for 29 structural sizing design variables and 6 shape design variables. Based on these numbers, it would require about 2242 CPU seconds to get nominal and perturbed aeroelastic responses for cruise and maneuver. However, using the modular sensitivity approach, we only need the partial derivatives of f_1 , f_2 , and f_3 . Individually, we need 57.56 CPU seconds to get the f_1' , 12.34 CPU seconds to get the f_2' , and 80.10 CPU seconds to get the f_3' . For the divergence derivatives, we need 107.50 CPU seconds to get $A'\theta_D$, and 2.34 CPU seconds to get $S'F_{aD}$. This totals up with a total time of 639 CPU seconds. Compared with the 2242 CPU seconds for an overall finite-difference approach, it is equivalent to a 74% saving in CPU time. Table 10 summarizes the above results.

3.3.5 Optimization Results

The complete design process requires 7 design cycles. Fig. 18 plots the weight history of the integrated design optimization for a subsonic transport aircraft. The gross weight of the aircraft is reduced from an initial 4.391 x 10^5 N to a final 4.150 x 10^5 N which is about a 5.5% reduction. The difference of 2.410 x 10^4 N is due to reduction of the structural wing weight multiplied by two and the reduction of the usable fuel weight. The initial and the final designs of the transport wing are summarized in Table 11. In the first column of this table are the initial design data. In the second column of this table are the final design data. We can see that the structural wing weight is decreasing from 2.779 x 10^4 N to 1.728 x 10^4 N, and the usable fuel weight is decreasing from 2.190 x 10^4 N to 1.876 x 10^4 N. The range of the initial design is 17% larger than the reference range. The reason for the difference between the initial range and the reference range is we fly at a lower Mach number which is 0.48 compared with a 0.78 Mach number of the reference aircraft. At the end of the design, the range is 1% higher than the reference range. The geometry design variables in the Table show that we have a smaller wing for the final design which is due to the initial range margin. The fact that the range constraint has a margin of 1% is indicative of slow convergence of the method, which is probable due to the poor initial guess. The design results should be viewed as preliminary. Refined design results will be presented in the future paper.

From Table 7, we see that the gross weight of the reference aircraft is 4.494 x 10^5 N which is about 7.7% higher than the one obtained from the final design which is again due to savings associated with the reduced Mach number.

Chapter 4

Concluding Remarks

This dissertation focuses on the processes of simultaneous structural and aerodynamic wing design as a prototype for design integration. We concentrate on the major difficulty associated with multidisciplinary design optimization processes, their enormous computational costs. Techniques for reducing this computational burden are presented.

The first technique is the development of efficient methods for the calculations of the derivatives of the flexibility matrix and the aerodynamic influence coefficient matrix. An adjoint method is used for the flexibility sensitivity, and a perturbation method is used for the aerodynamic sensitivity.

The second method is the implementation a sequential optimization algorithm that employs approximate analysis methods. In the sailplane wing design, a linear approximation to the elastic lift distribution allows us to calculate the objective function without an exact aeroelastic analysis for each design analysis. In the transport wing

design, a linear approximation to the drag of the elastic wing allows us to calculate the range without a full aerodynamic and aeroelastic analyses.

The last method is a modular sensitivity analysis. This modular approach, corresponds to the abstraction of a system as an assembly of interacting black boxes. This method was developed for calculating system sensitivity without modifying discipline black-box software packages. Consequently, this method is particularly suitable for a large engineering design environments, in that we can integrate different disciplines into team work while keeping their original independence. Within this framework, aeroelastic sensitivities can be computed without the expensive calculation of the derivatives of the flexibility matrix and the aerodynamic influence coefficient matrix.

The next stage of the integrated design research will add a control system in the design optimization which results in a coupled problem of structure, aerodynamics and control design. With this change, we need to investigate the coupling effects among these disciplines, and generate a new set of coupled nonlinear equations for the modular sensitivity analysis. We also plan to introduce a more realistic design problem including optimizing airfoil shape, flying at a transonic Mach number, and including additional structural constraints (e.g. buckling, flutter, frequencies, interlaminar stresses for composite material). This additional complexity will require more efficient algorithms to further reduce the computational costs.

References

[1] Sobieszczanski-Sobieski, J.; Barthelemy, J. F.; and Giles, G. L.: "Aerospace Engineering Design by Systematic Decomposition and Multilevel Optimization," International Council of Aeronautical Science, 14th Congress, Paper No. ICAS-84-4.7.3, 1984

[2] McGeer B. T.: "Wing Design for Minimum Drag with Practical Constraints" Journal of Aircraft, Vol. 21, No. 11, pp. 879-886, 1988

[3] Sobieszczanski-Sobieski, J. (Editor) : "Recent Experiences in Multidisciplinary Analysis and Optimization" NASA CP-2327, 1984

[4] Barthelemy, J. F. (Editor) : "Recent Experiences in Multidisciplinary Analysis and Optimization" NASA CP-3031, 1989

[5] Haftka, R. T.: "Structural Optimization with Aeroelastic Constraints a Survey of US Applications" International Journal of Vehicle Design, Vol. 7, pp. 381-392, 1986

[6] Shirk, M. H.;, Hertz, T. J; and Weisshar, T. A.: "A Survey of Aeroelatic Tailoring - Theory, Practice, and Promise" Journal of Aircraft, Vol. 23, No. 1, pp. 6-18, Jan. 1986

[7] Sobieszczanski-Sobieski, J.; Haftka, R. T.: "Interdisciplinary and Multilevel Optimum Design" Proceedings of the NATO Advanced Study Institute on Computer Aided Optimal Design:Structural and Mechanical Systems, Edited by C. A. Mota Soares, Springer-Verlag 1987

[8] Sobieszczanski-Sobieski, J.: "A Linear Decomposition Method for Large Optimization Problems" NASA TM-83248, 1982

[9] Sobieszczanski-Sobieski, J.; Barthelemy, J. F.: "Improving Engineering System Design by Formal Decomposition, Sensitivity Analysis and Optimization" Pro-

ceedings of International Conference of Engineering Design, Hamburg, West Germany, pp. 314-321, 1985

[10] Sobieszczanski-Sobieski, J.; James, B. B.; and Riley, M. F.: "Structural Optimization by Generalized Multilevel Optimization" NASA TM-87605, 1985

[11] Sobieszczanski-Sobieski, J.; James, B. B.; and Dovi, A.: "Structural Optimization by Multilevel Decomposition" AIAA Journal, Vol. 23, No. 11, 1985, pp. 1775-1782

[12] Mesarovic, M. D.; Macko. D.; and Takahara, Y.: "Theory of Hierarchical Multilevel Systems" Academic Press, N.Y. 1970

[13] Wrenn, G. A.; Dovi A.R.: "Multilevel/Multidisciplinary Optimization Scheme for Sizing a Transport Aircraft Wing" NASA CR-178077, 1986

[14] Strauch, G. J.: "Integrated Multidisciplinary Design of a Sailplane Wing" MS Thesis VPI&SU, 1985

[15] Grossman, B.; Strauch, G. J.; Eppard, W. M.; Gurdal, Z.; and Haftka, R. T.: "Combined Aerodynamic/Structural Design of a Sailplane Wing" Journal of Aircraft, Vol. 25, No. 9, pp. 855-860, 1988

[16] Haftka, R. T.; Grossman, B.; Eppard, W. M.; and Kao, P. J.: "Efficient Optimization of Integrated Aerodynamic-Structural Design," To be published in International Journal for Numerical Methods in Engineering

[17] Sobieszczanski-Sobieski, J. : "On the Sensitivity of Complex, Internally Coupled System" AIAA/ASME/ASCE/AHS 29th Structures, Structural Dynamics and Materials Conference, Williamsburge, Va. April 1988, AIAA Paper No. CP-88-2378

[18] Haftka, R. T.; Grossman, B.; Kao, P. J.; Polen, D. M. and Sobieszczanski-Sobieski, J: "integrated Aerodynamic-Structural Design of a Forward-Swept Transport Wing, " Proc. of Second NASA/Air Force Symposium on Recent Experiences in Multidisciplinary Analysis and Optimization, Sept. 28-30, 1988

[19] Eppard, W. M.: "Integrated Aerodynamic-Structural Design Optimization" MS Thesis VPI&SU, 1987

[20] Polen, D. M.: "Integrated Aerodynamic-Structural Design of a Forward-Swept Transport Wing" MS Thesis VPI&SU, 1989

[21] Haftka, R. T. and Starnes, J. H. Jr.: "WIDOWAC: Wing Design Optimization with Aeroelastic Constraints - Program Manual" NASA TM X-3071, 1974

[22] Schmit, L. A. and Farshi, B.: "Some Approximation Concepts for Structural Synthesis" AIAA Journal, Vol. 12, No. 5, 1974, pp. 692-699

[23] Grandhi, R. V.; Thareja, R. and Haftka, R. T.: "NEWSUMT-A: A General Purpose Program for Constrained Optimization Using Constraint Approximations" ASME J. Mech.,Trans. & Automation in Design, Vol. 107, pp. 94-107 March 1985

[24] Sewall, W. G.; McGhee, R. J.; Viken, J. K.; Waggoner, E. G., Walker, B. S; and Millard, B. F.: "Wind Tunnel Results for a High-Speed, Natural Laminar-Flow Airfoil Designed for General Aviation Aircraft" NASA TM-87602, 1987

[25] Tuttle, M. H. and Maddalon, D. V.: "Laminar Flow Control (1976-1982) : a Selected, Annotated Bibliography" NASA TM-84496, 1982

Table 1. Summary of CPU Times on IBM 3090 to Calculate A matrix for Sailplane Wing (in Seconds)

Panels	Finite Difference CPU sec	Perturb CPU sec	Percent savings
80	5.8	4.6	20.7
120	20.7	13.6	34.3
160	54.3	30.3	44.2
200	116.8	56.4	51.7

Table 2. Comparison of CPU Times on IBM 3090 to Calculate Derivatives of Lift Coefficients for Sailplane Wing (in Seconds)

	S	$\partial S/\partial x$	Others	Total
Exact S	47.4	0	$\simeq$ 31.2	78.6
Approx. S	0	10.3	$\simeq$ 31.2	41.5

Table 3. Design Variables of the Sailplane Wing Design

3 Performance Design Variables	1. Angle of attack during turn
	2. Angle of Attack during cruise
	3. Radius of turn
6 Geometric Design Variables	4. Twist angle at the break
	5. Twist angle at the root
	6. Chord length at the root
	7. Chord length at the break
	8. Chord length at the tip
	9. Distance to the break
32 Structural Design Variables	10-17. Spar cap thickness
	18-25. Spar web thickness
	26-41. Skin thickness

Table 4. Design Constraints of the Sailplane Wing Design

3 Stall Constraints During Turn	1. No Stall at root
	2. No stall at break
	3. No stall at tip
3 Performance Constraints	4. Bank angle less than 50 deg.
	5. Climb speed greater than zero
	6. Minimum divergence speed
81 Structural Constraints	7-14. Maximum spar cap strain
(43 m/sec, 5.9g)	15-22. Maximum shear stress
	23-86. Maximum strain in skin

Table 5. Design Results for Sailplane Wing (0.9m/s thermal)

	Iterated Sequential	Integrated Design	Weight Minimization
Cross-Country speed (m/sec)	2.80	2.83	2.80
Wing Mass (Kg)	16.6	15.4	14.0
Chord Lengths (cm)			
Root	110	108	101
Break	110	105	94
Tip	45	44	40
Break Length (cm)	313	285	291
Relative Twist(deg)			
Break	0.94	1.27	0.16
Tip	-0.01	0.74	-0.01
Aspect Ratio	14.3	15.1	16.5
Wing Area (sq.m)	12.7	12.1	11.0

Table 6. Derivative of θ w.r.t. Skin Thickness by the Modular and Overall Finite-Difference Approach for Transport Wing

Load Set No.	Modular Approach	Finite-Difference
7	-6.4654321E-04	-6.4655011E-04
8	-8.1169167E-05	-8.1169698E-05
9	2.0794906E-04	2.0795188E-04
10	3.8526983E-04	3.8527484E-04
11	9.2402373E-04	9.2403512E-04
12	-3.1925238E-04	-3.1925594E-04

Table 7. Reference Aircraft Design Specifications

Weight, N:		
	W_p	1.368×10^5
	W_{RS}	2.852×10^5
	W_{RW}	3.020×10^4
Wing:		
	Aspect Ratio	14
	Area,m^2	83.98
	Span, m	34.29
	Thickness, %	12
	Sweep at c/4, deg.	15
	Taper Ratio	.25
Horizontal Tail Area,m^2		11.71
Vertical Tail Area,m^2		17.74
Average Cruise:		
	Mach No.	.78
	Lift Coeff.	.672
	L/D (Lift to Drag Ratio)	20.7
	c′ (Specific Fuel Consumption)	.430
Cruise Altitudes:		
	Start/End, m	12300/12600

Table 8. Design Variables of the Forward-Swept aircraft Design

8 Geometric Design Variables	1. Chord length at the root
	2. Chord length at the break
	3. Chord length at the tip
	4. Distance to the break
	5. Distance from break to tip
	6. Swept angle at the break
	7. Twist angle at the break
	8. Twist angle at the root
2 Performance Design Variables	9. Dynamic pressure at cruise
	10. Usable fuel weight
29 Structural Design Variables	11-34. Panel thicknesses
	35-38. Spar cap areas
	39. Ply orientation

Table 9. Design Constraints of the Forward-Swept aircraft Design

305 Structural Constraints	1-228. Maximum strain in composite skin
	229-304. Maximum spar cap stresses
	305. Divergence dynamic pressure
2 Performance Constraints	306. Range
	307. Enough volume for fuel

Table 10. Comparison of CPU Times on IBM 3090 to Calculate Aeroelastic Sensitivities for Transport Wing (in Seconds)

	Modular Approach	Finite-Difference Approach
f_1'	115.12	No Need
f_2'	24.68	No Need
f_3'	160.20	No Need
$A'\theta_D$	107.50	No Need
$S'F_{aD}$	2.34	No Need
A	224.25	2245.40
S	4.91	176.76
Total	639.29	2422.16

Table 11. Initial and Final Designs for Transport Wing

	Initial Design	Final Design
Gross Weight (N)	4.391×10^5	4.150×10^5
Wing Weight (N)	2.779×10^4	1.728×10^4
Usable Fuel Weight (N)	2.190×10^4	1.876×10^4
Range Margin from Reference	17%	1%
Chord Lengths (m)		
Root	6.916	5.912
Break	3.765	3.218
Tip	1.725	1.234
Distance from Root to Break (m)	5.754	4.918
Distance from Break to Tip (m)	12.250	10.443
Sweep Angle(deg.)	63.9	71.2
Elastic Twist(deg.)	.33	.46
Elastic Disp.(m)	.89	.36

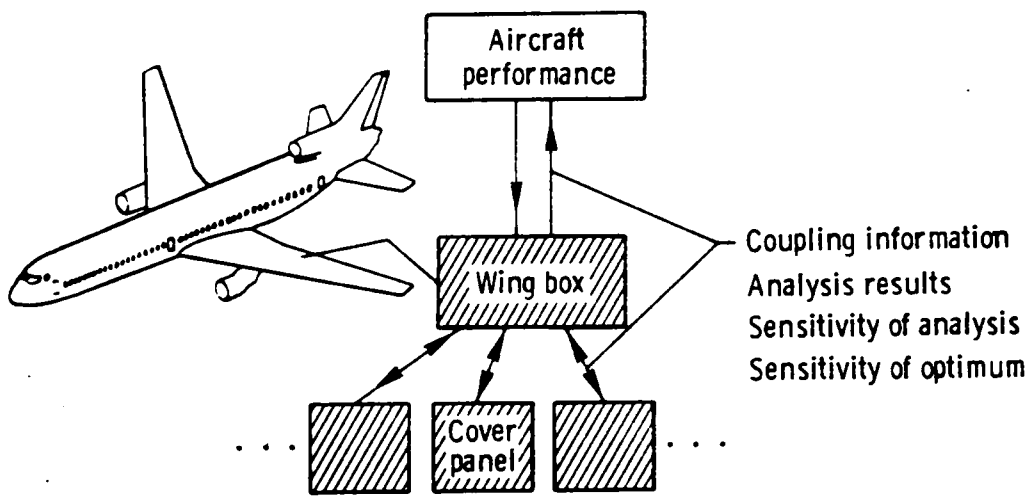

Figure 1. Aircraft and a Schematic of its Multilevel Optimization (From Ref. 13)

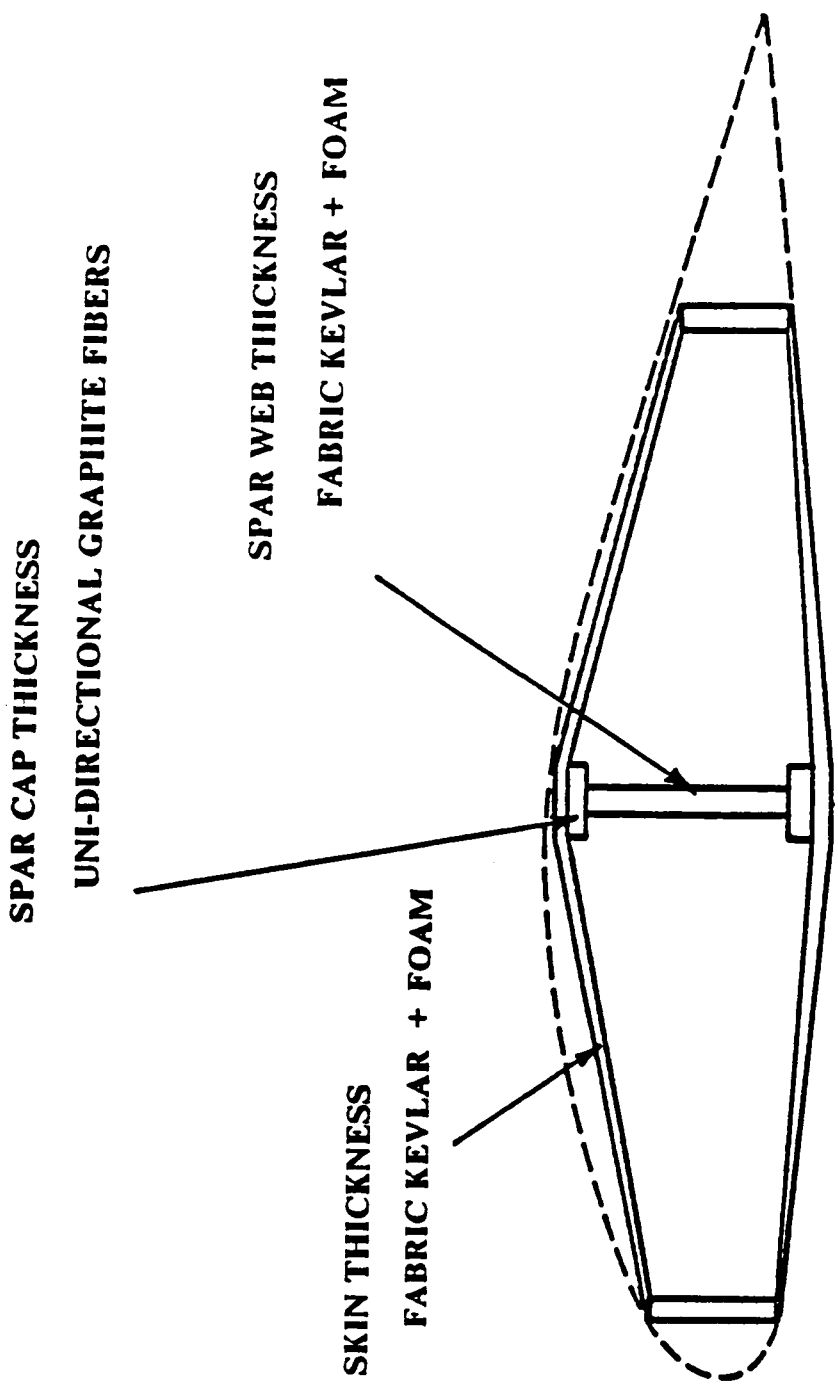

Figure 2. Structural Details of the Sailplane Wing

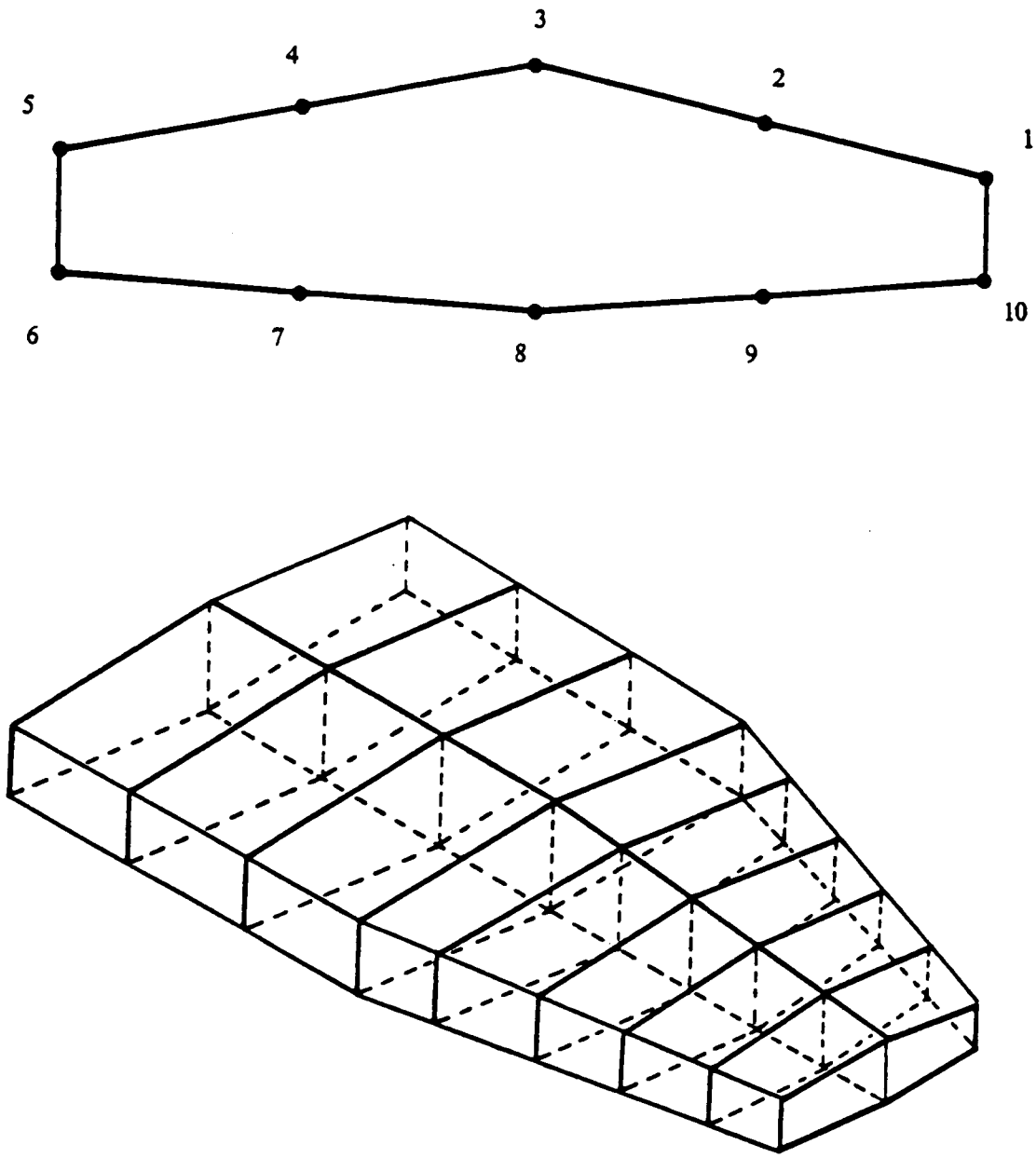

Figure 3. Sailplane Structural Wing Sections and Nodes

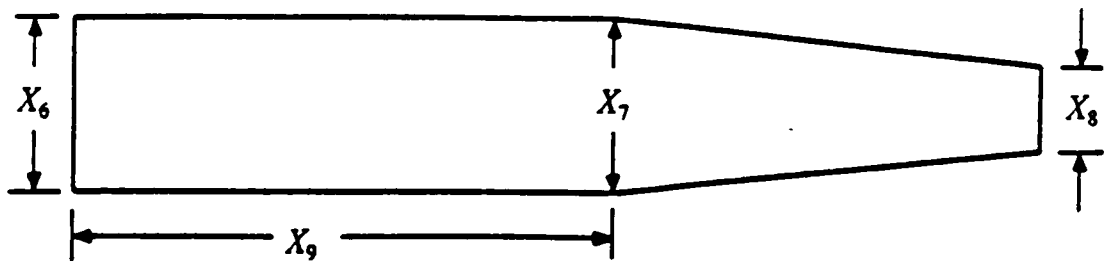

Figure 4. Sailplane Planform Geometry Variables

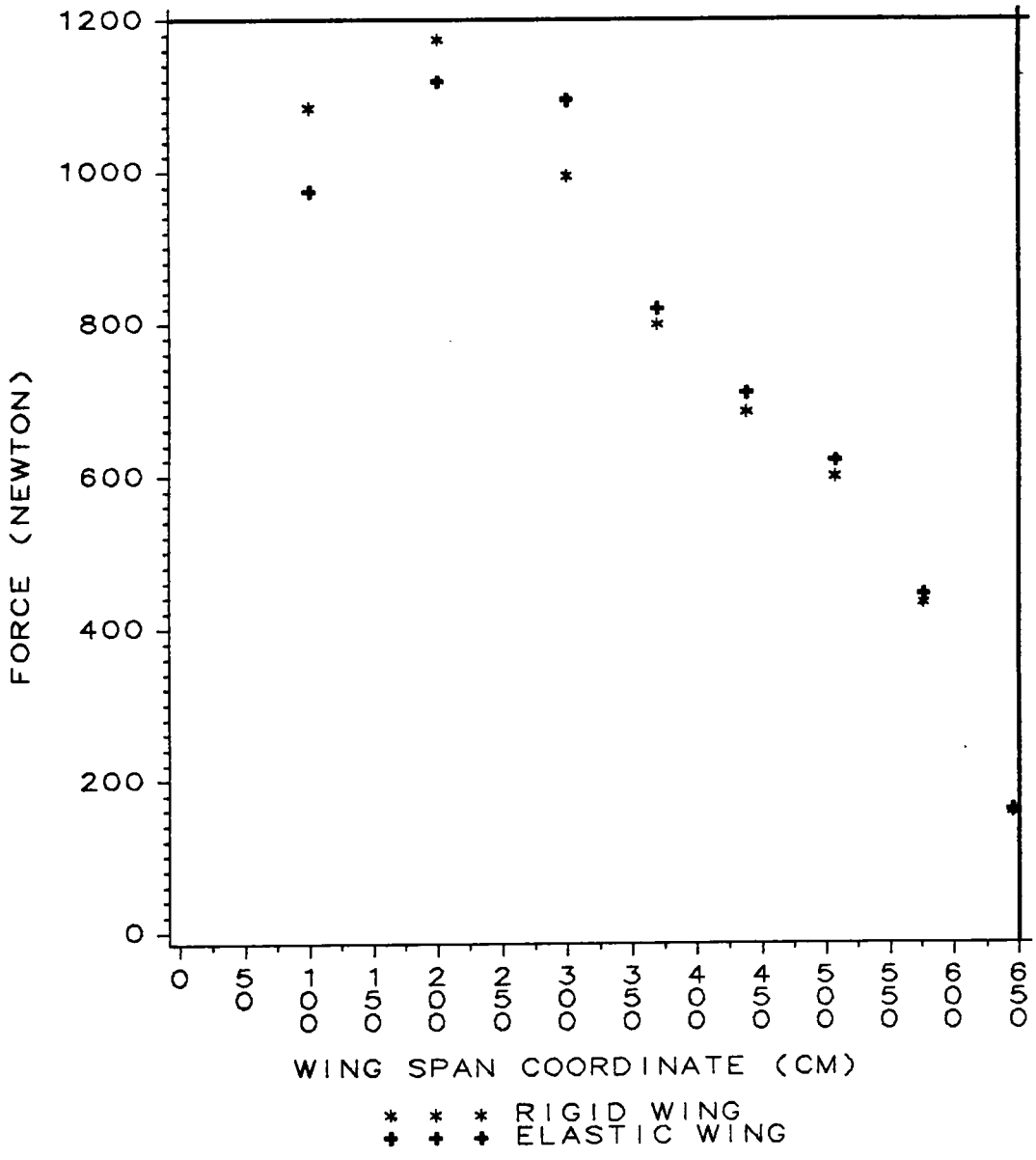

Figure 5. Typical Loads for the Rigid and Elastic Sailplane Wing

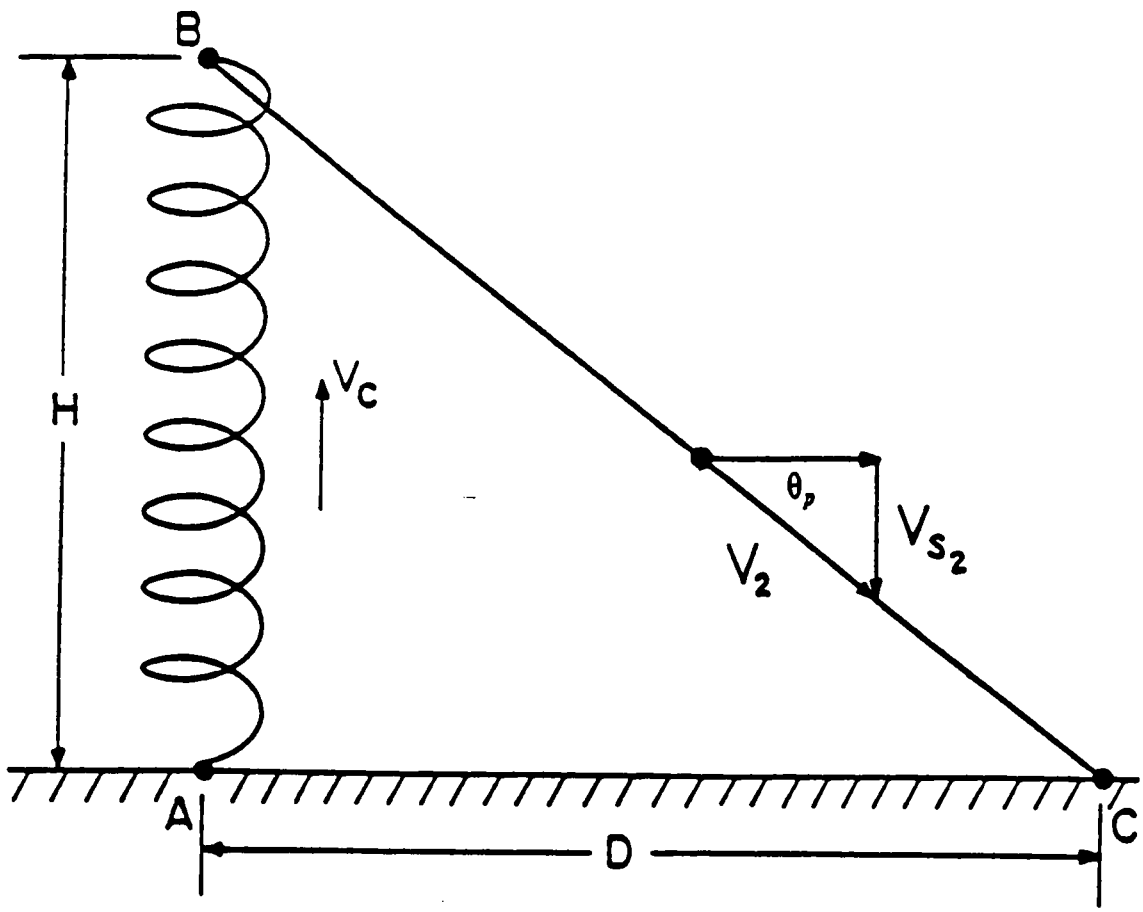

Figure 6. Sailplane Mission Profile

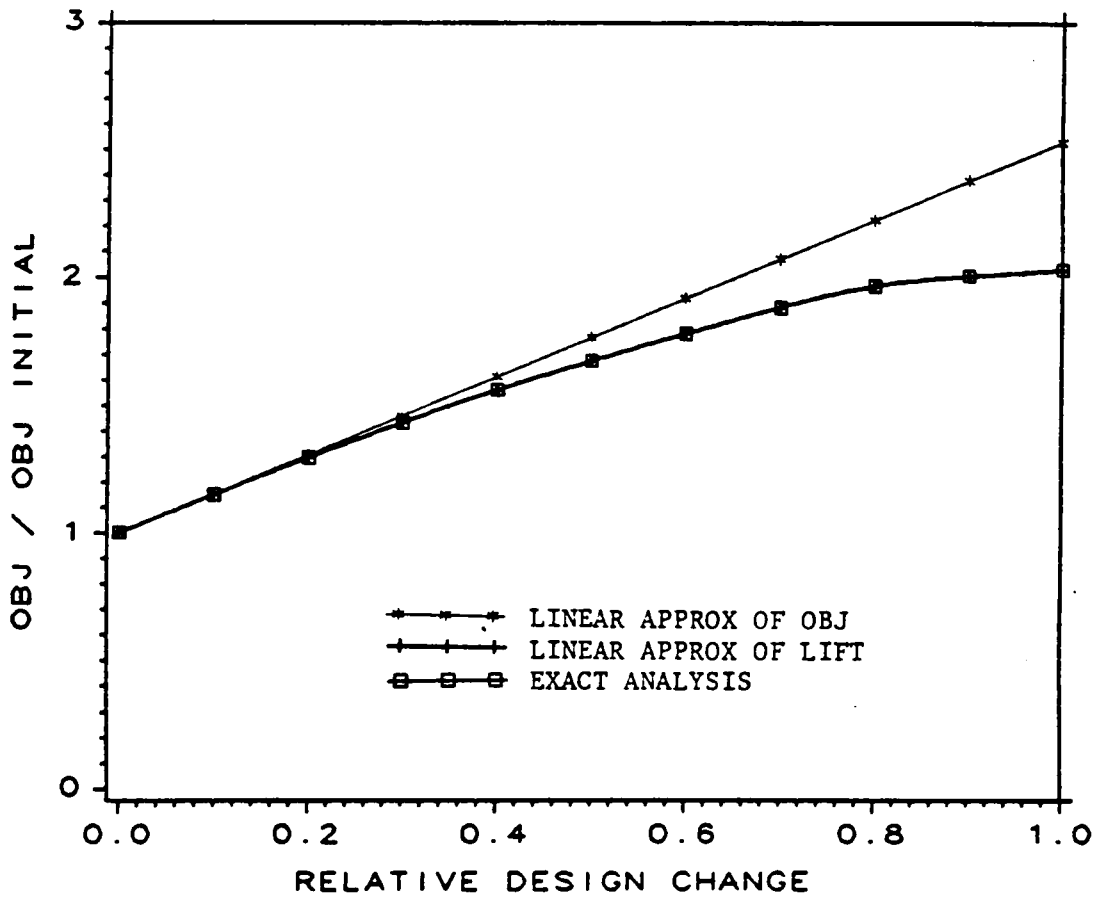

Figure 7. Comparison of Approximations to Objective Function (Cross Country Speed)

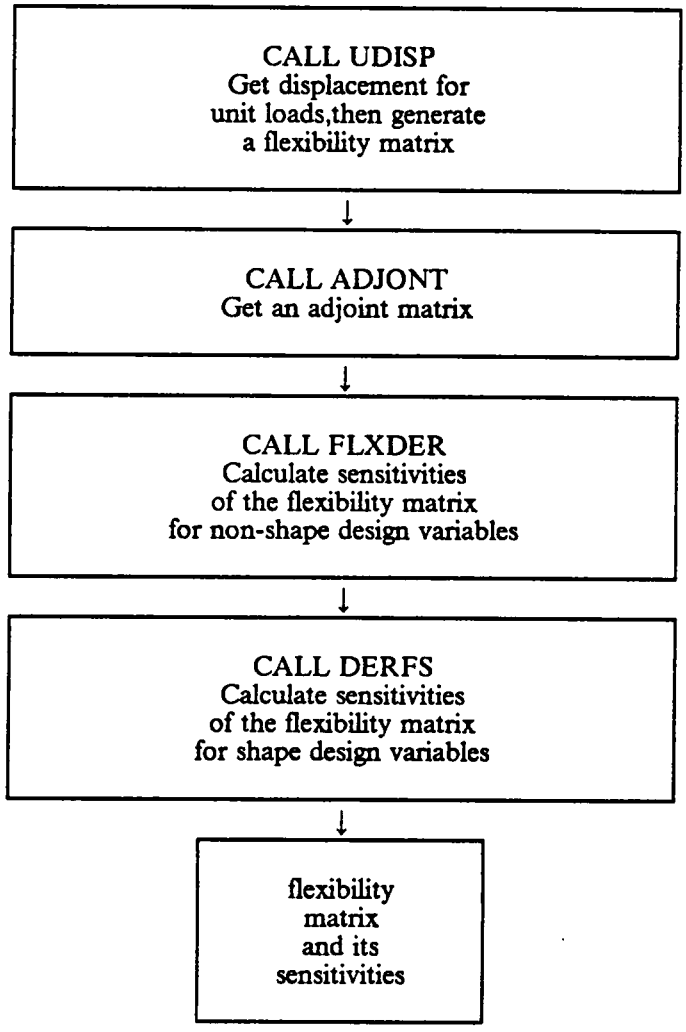

Figure 8. Flow Chart of Flexibility Module in Sailplane Wing Design Problem

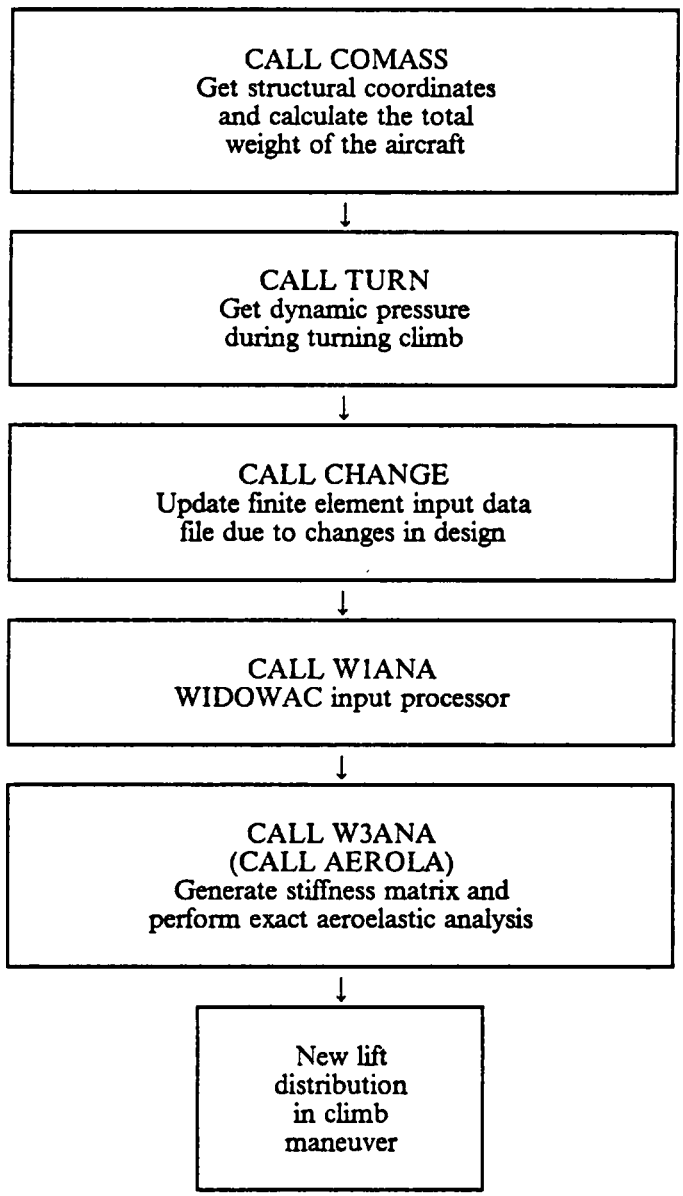

Figure 9. Flow Chart of Aeroelastic Module in Sailplane Wing Design Problem

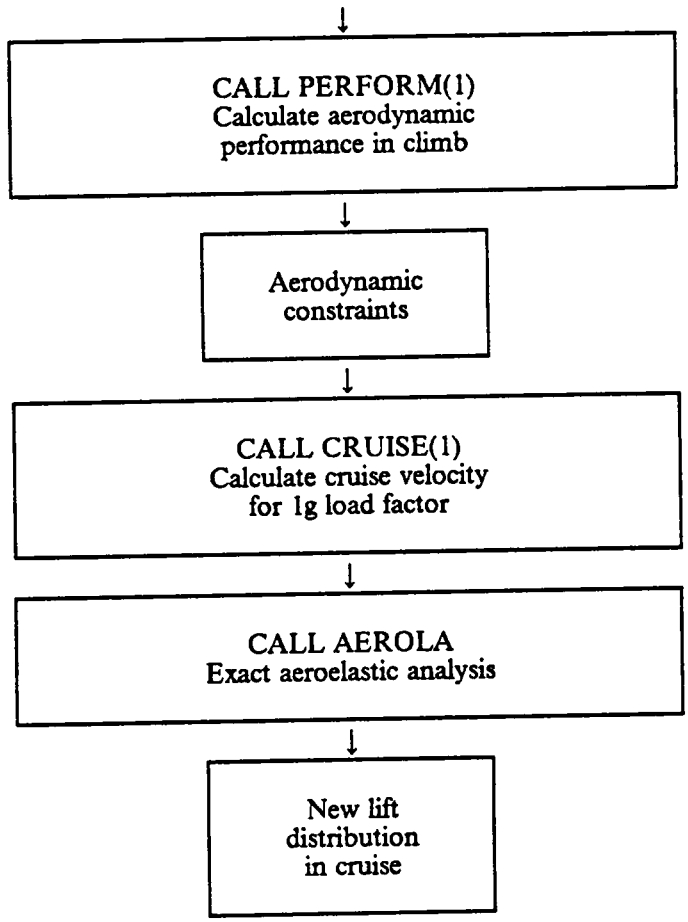

Figure 9. Flow Chart of Aeroelastic Module in Sailplane Wing Design Problem (continued)

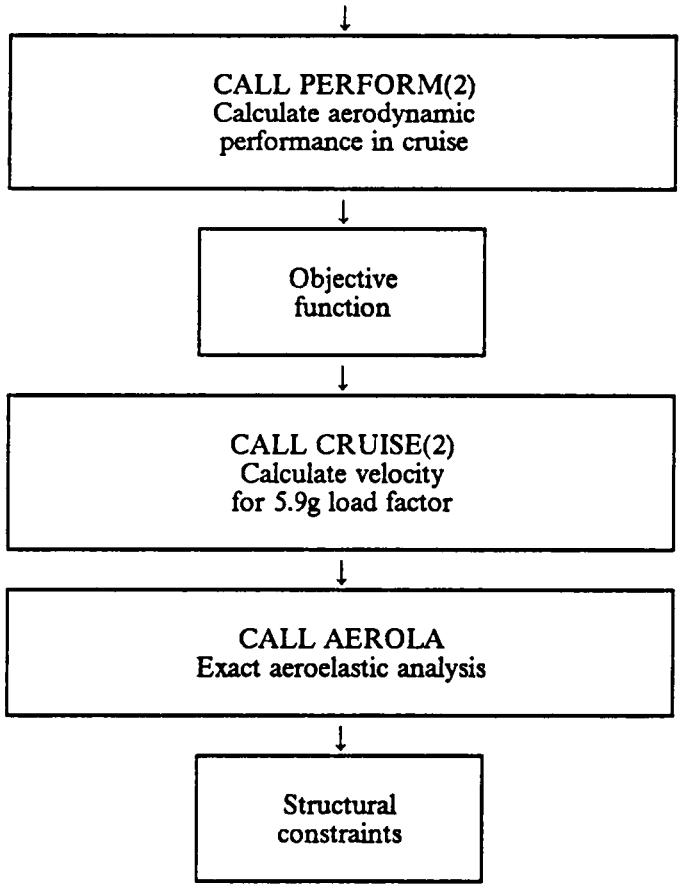

Figure 9. Flow Chart of Aeroelastic Module in Sailplane Wing Design Problem (concluded)

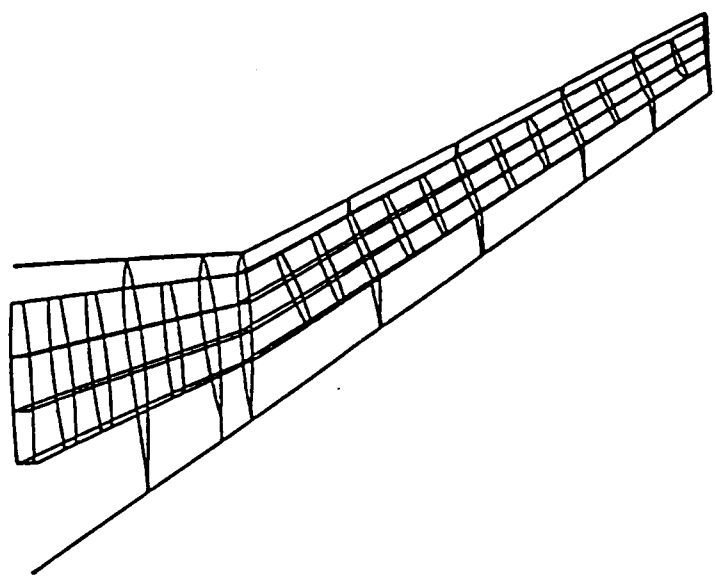

Figure 10. Structural model of Forward-Swept Transport Wing

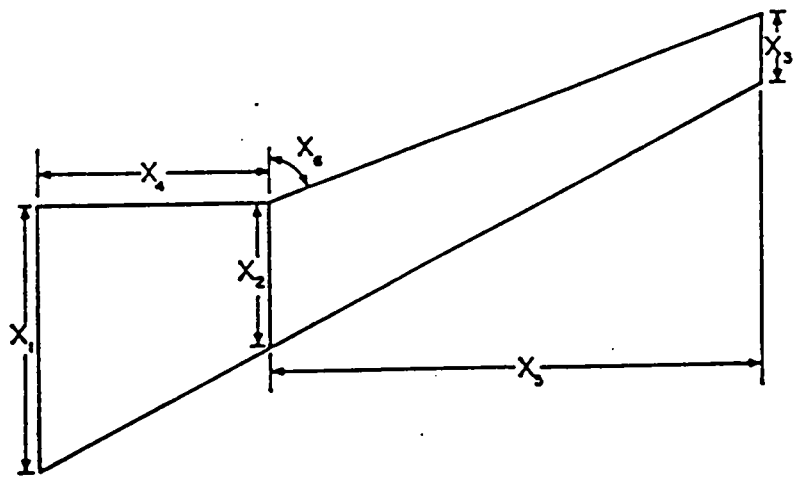

Figure 11. Planform Design Variables

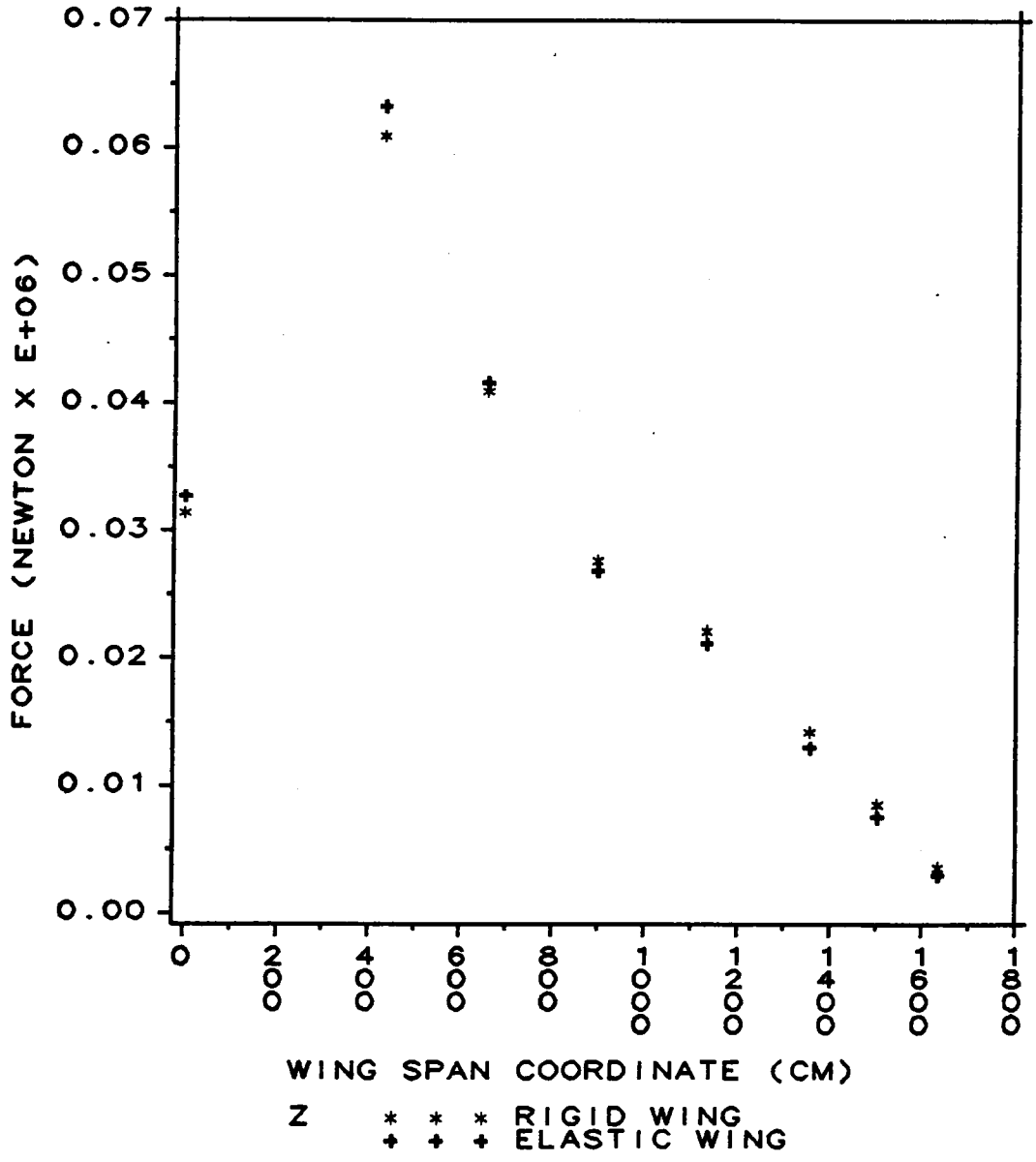

Figure 12. Typical Loads for Rigid and Elastic Transport Wing with a Nose-Down Twist

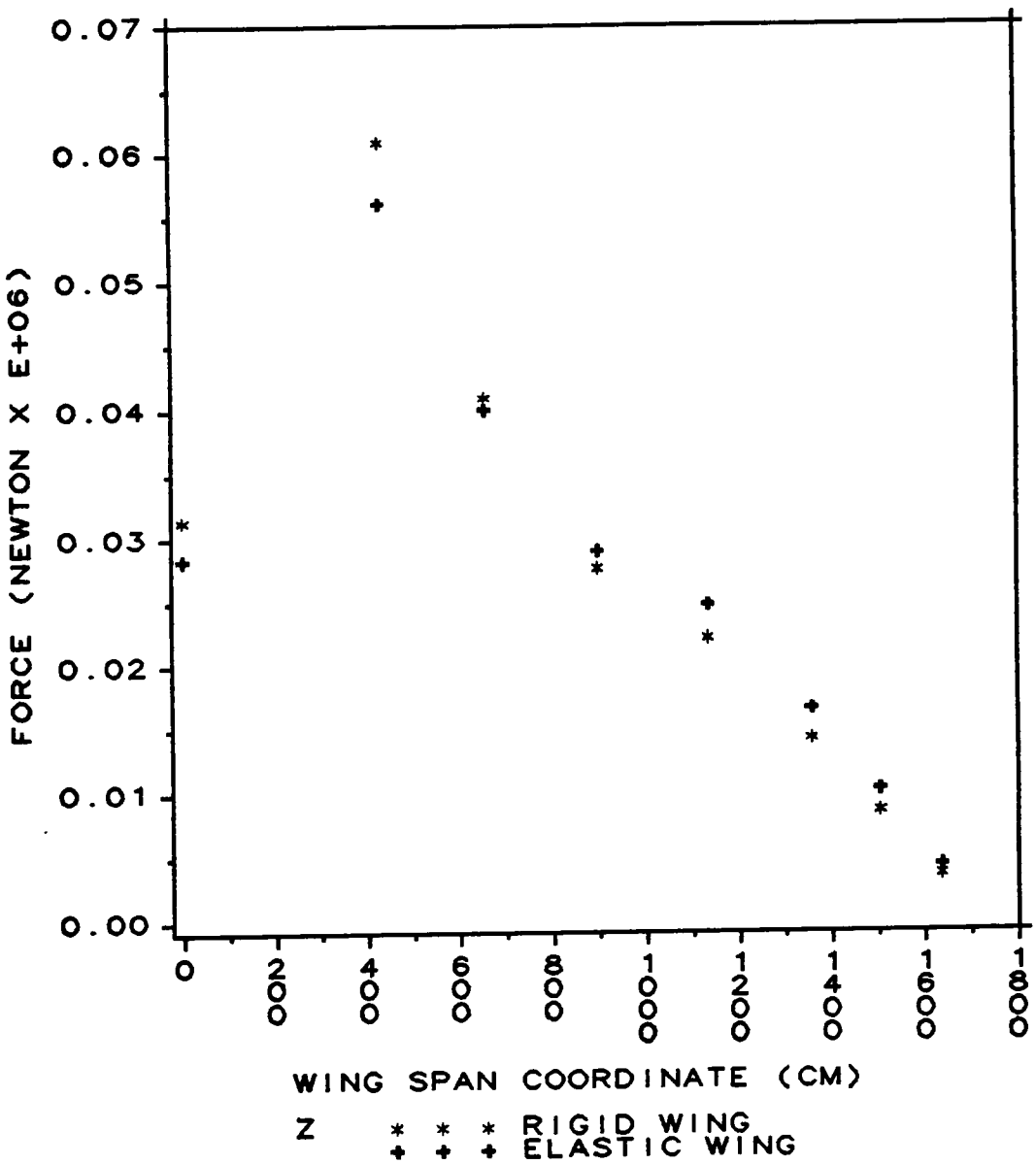

Figure 13. Typical Loads for Rigid and Elastic Transport Wing with a Nose-Up Twist

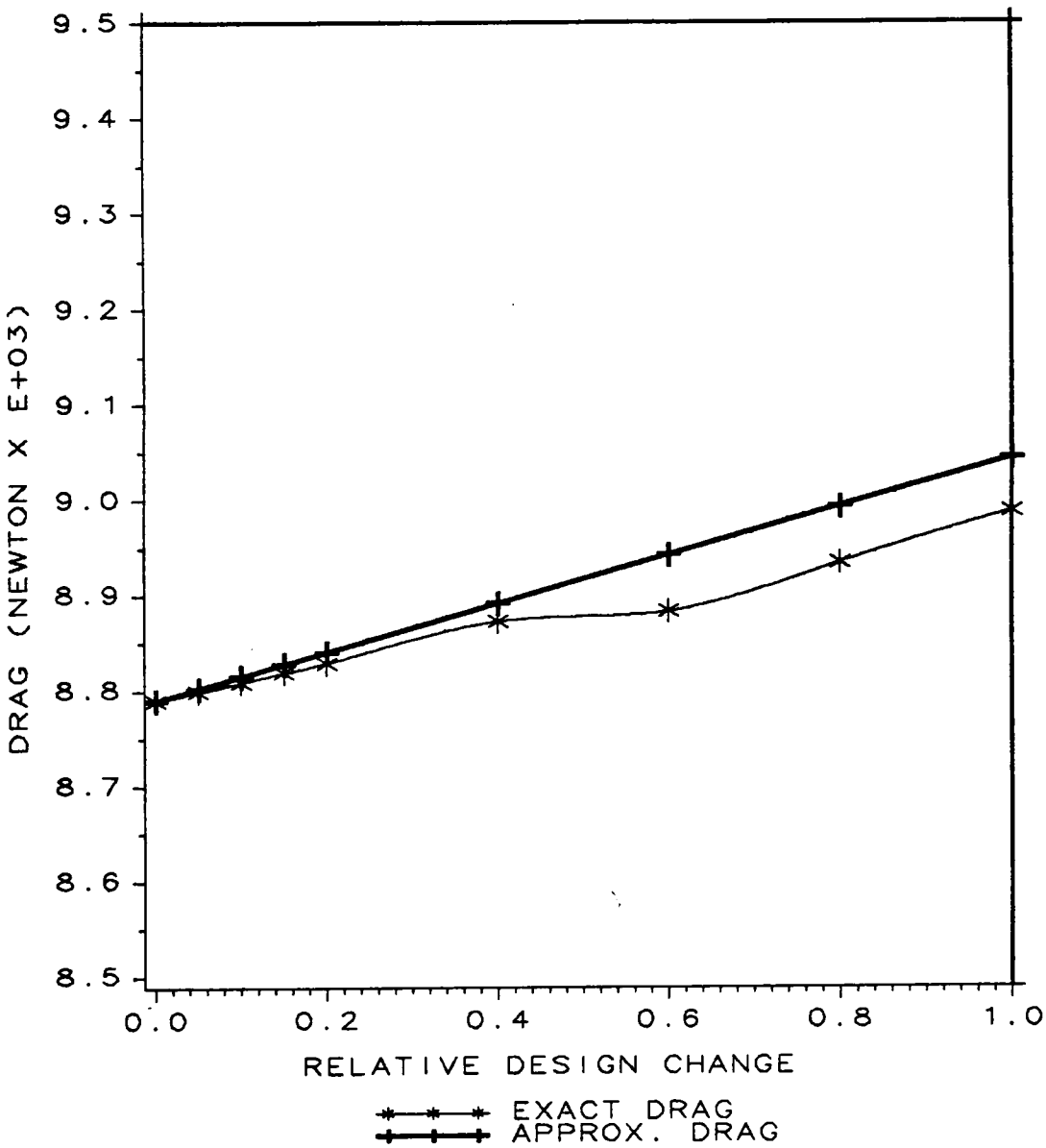

Figure 14. Comparison of Approximation to Drag

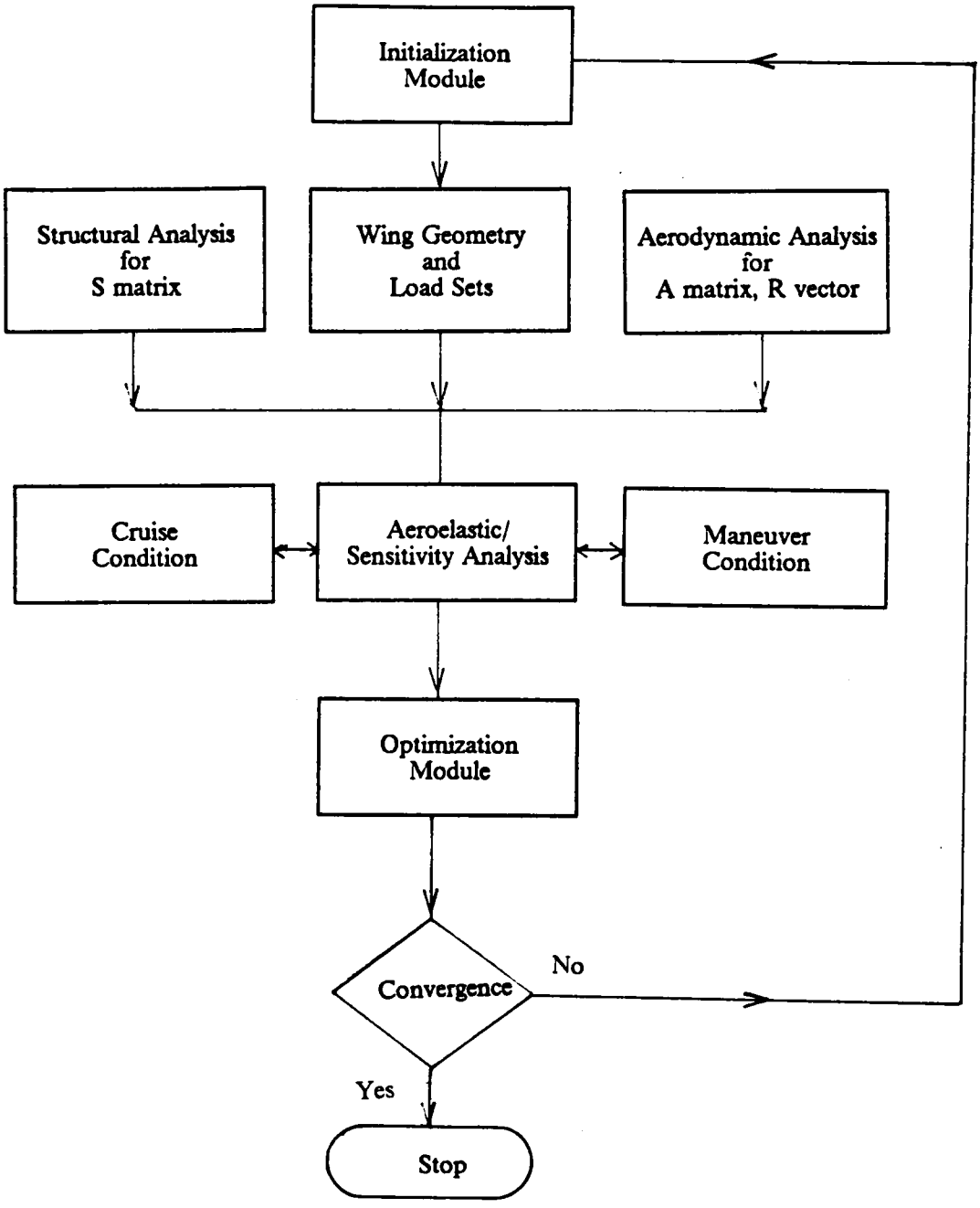

Figure 15. Flow Chart of the Design Procedure

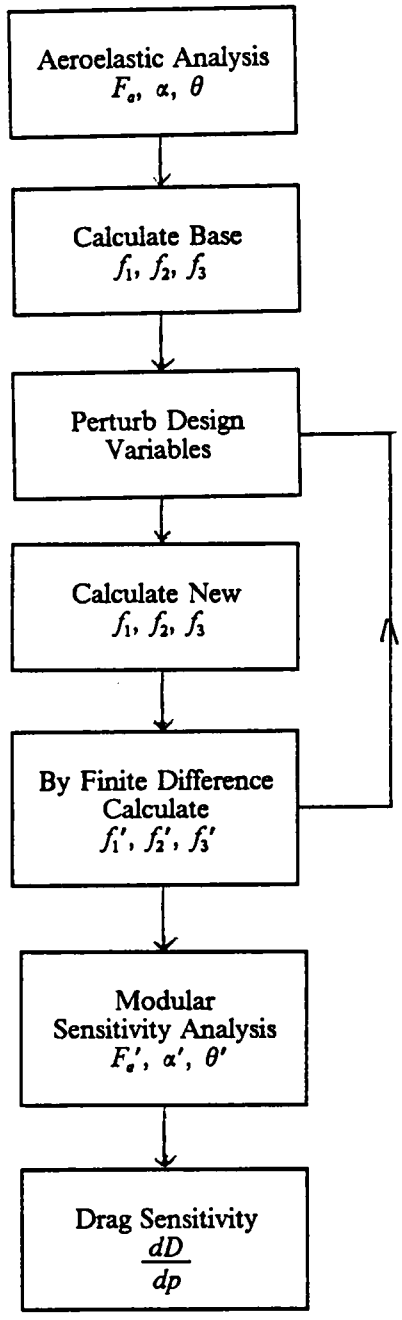

Figure 16. Flow Chart for Aeroelastic Sensitivity Analysis - Cruise

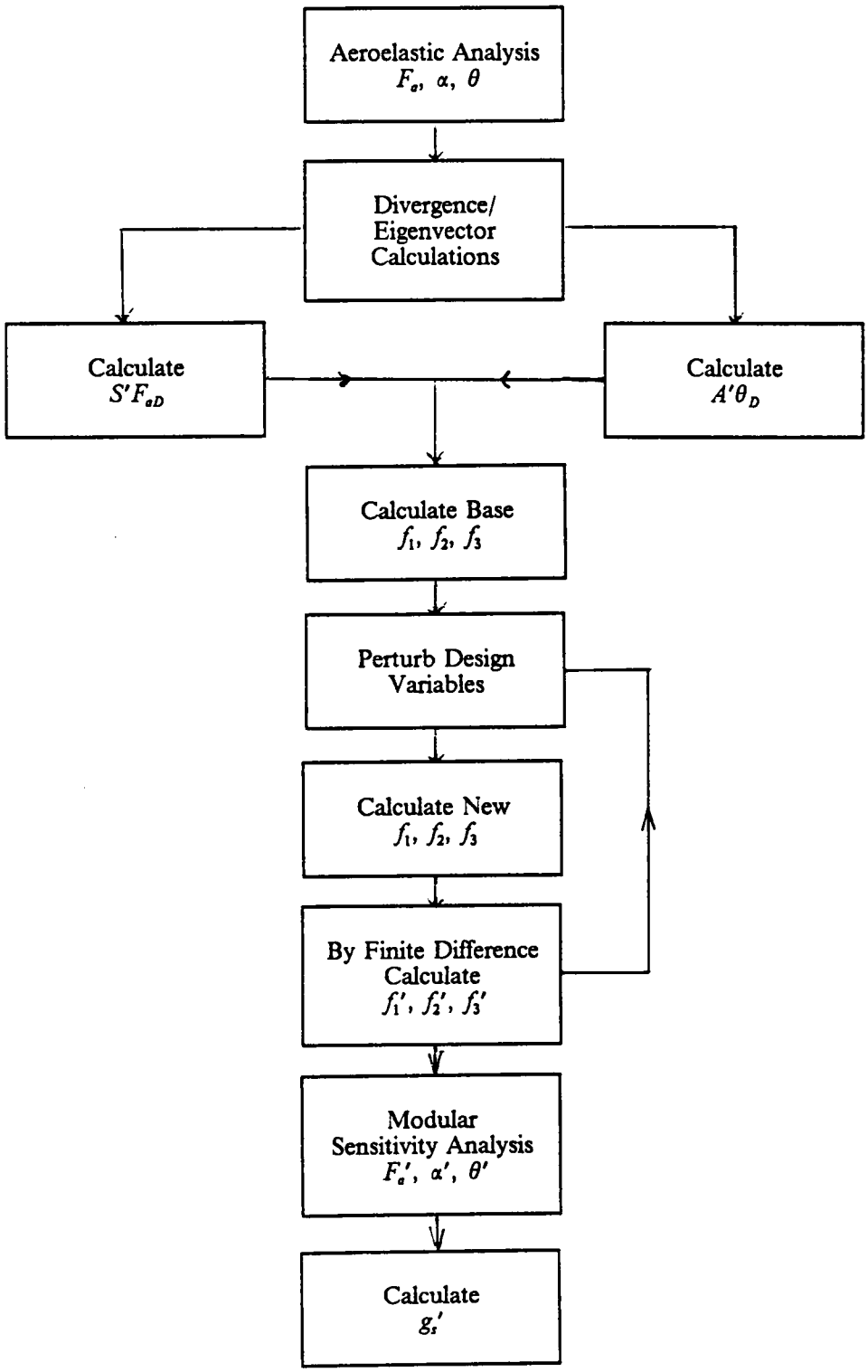

Figure 17. Flow Chart for Aeroelastic Sensitivity Analysis - Maneuver plus structural constraint sensitivity

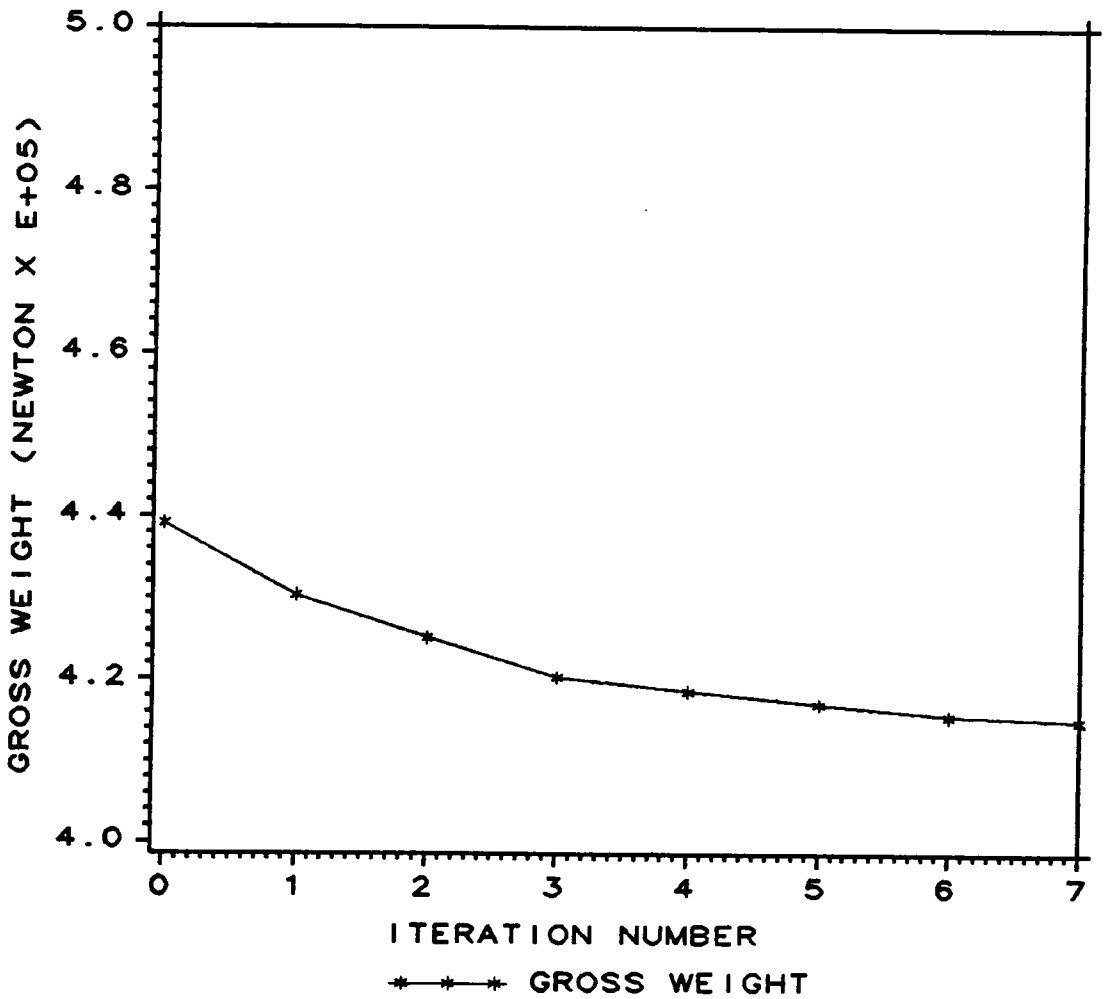

Figure 18. Weight Convergence

Appendix

Range Calculation

If we neglect the small effect of changes in elastic deformation due to change in weight, we can write the drag D of the aircraft as

$$D = qS_aC_D(C_L) \tag{1}$$

where q is the dynamic pressure, S_a is the wing span, C_D is the drag coefficient which is a function of the cruise lift coefficient C_L is given as

$$C_L = \frac{W}{qS_a} \tag{2}$$

where W is the weight of the aircraft. To find the optimum dynamic pressure q_m (and hence optimal altitude) we differentiate D with respect to q and set to zero as

$$\frac{dD}{dq} = S_a C_D + q s_a \frac{dC_D}{dC_L} = 0 \tag{3}$$

Differentiating Eq.(2) and substituting it into Eq.(3), yields

$$\frac{dD}{dq} = S_a C_D - \frac{dC_D}{dC_L}\frac{W}{q} = 0 \tag{4}$$

or

$$q_m = \frac{W}{S_a}\frac{dC_D}{dC_L}\frac{1}{C_D} \tag{5}$$

Finally Eq.(1) is written for the minimum drag D_m by using q_m and C_{Lm} (the corresponding optimum lift coefficient) as

$$D_m = W\frac{dC_D}{dC_L}(C_{Lm}) \tag{6}$$

which indicates that D_m is proportional to W.

For an elastic wing, we assume that the minimum drag is still proportional to the weight, calculating the constant of proportionality, $\bar{D}$ at a weight W_0, corresponding to half-fuel condition

$$D_m = \bar{D} W_0 \tag{7}$$

The rate of change of aircraft weight due to burning fuel is

$$\frac{dW}{dt} = -c'T = -c'D = -c'\bar{D}W \tag{8}$$

where c' is the thrust specific fuel consumption and T is the thrust. Integrating Eq.(8) between the initial time t_i and final time t_f we get

$$\ln\left(\frac{W_i}{W_f}\right) = -c'\bar{D}(t_f - t_i) \tag{9}$$

Since we assume the aircraft is flying at a constant speed V_c , the cruise range R_g is given as

$$R_c = V_c(t_f - t_i) = \frac{V_c}{c'\bar{D}} \ln\left(\frac{W_i}{W_f}\right) = \frac{V_c W_0}{c' D_0} \ln\left(\frac{W_i}{W_f}\right) \tag{10}$$

where D_0 is the value of D_m corresponding to W_0 .

The vita has been removed from the scanned document